

# **Development of an Autonomous OmniCopter Aerial Vehicle**

by

Florentin von Frankenberg

Bachelor of Mechanical Engineering and Management (Hons), University of Ontario  
Institute of Technology, 2010

A THESIS SUBMITTED IN PARTIAL FULFILLMENT OF THE  
REQUIREMENTS FOR THE DEGREE OF

Master of Applied Science

in

The Faculty of Engineering and Applied Science

Mechanical Engineering

Supervisor(s): Scott Nokleby, Faculty of Engineering and Applied Science  
Examining Board: Remon Pop-Iliev, Faculty of Engineering and Applied Science  
External Examiner: Jing Ren, Faculty of Engineering and Applied Science

THE UNIVERSITY OF ONTARIO INSTITUTE OF TECHNOLOGY

August 2016

©Florentin von Frankenberg 2016

# Abstract

Traditional multirotors and helicopters control translational movement by changing the orientation of the entire vehicle. This limits the effectiveness of such vehicles in applications as a mobile manipulator base. In these applications it is often necessary to fly in proximity to large structures where unpredictable aerodynamic conditions exist. In order to maintain precise control of position it is necessary to counteract disturbance forces quickly, and, due to the delay induced by rolling and pitching the entire vehicle, traditional multirotors and helicopters have a limited ability to maintain position precisely. Additionally, a mobile base must be capable of resisting arbitrary combinations of force and torque resulting from use of a manipulator arm. This is also not possible for traditional multirotors and helicopters.

A novel Unmanned Aerial Vehicle (UAV) concept is presented which features the addition of four rotors directed orthogonally to the main lift rotors of a traditional quadrotor design. These rotors allow de-coupling of orientation from translational movement.

Tests done on a physical prototype demonstrated improvements in disturbance rejection and an ability to roll or pitch up to 20 degrees independently of translational movement, including the ability to move backwards at an angle. This type of motion is impossible for a traditional multirotor vehicle.

By adding a goal velocity term to the control algorithm, the ability to match the position and velocity of a moving target was demonstrated. This, combined with the ability to control orientation independently of the direction of flight, gives the OmniCopter the ability to land on or dock with a moving target.

# Acknowledgements

First of all, I would like to express my appreciation to my supervisor Dr. Scott Nokleby for his direction, encouragement, and most of all his enduring patience throughout this project. I would also like to acknowledge Dr. Remon Pop-Iliev for his involvement in the genesis of the larger AMS project, which this work is a part of, and Tony Baltovski for his help initially with the start of my work.

I would like to thank my lab colleagues and friends, Michael Hosmar and Michael Wrock, for their camaraderie, frequent assistance, and thoughtful input at many stages throughout this work.

# Table of Contents

<b>Abstract</b>	ii
<b>Acknowledgements</b>	iii
<b>Table of Contents</b>	vi
<b>List of Tables</b>	vii
<b>List of Figures</b>	x
<b>Glossary</b>	xi
<b>1 Introduction</b>	1
1.1 Background . . . . .	2
1.2 Literature Survey . . . . .	4
1.2.1 Overview . . . . .	4
1.2.2 Classification of UAVs . . . . .	4
1.2.3 Aerial Inspection . . . . .	5
1.2.4 UAV Modelling and Control . . . . .	7
1.2.5 Vehicle Aerodynamics . . . . .	12
1.2.6 Environmental Aerodynamics . . . . .	13
1.2.7 Grasping and Perching . . . . .	15
1.2.8 Aerial Manipulation . . . . .	17

1.2.9	Novel UAV Platforms . . . . .	18
1.2.10	Summary . . . . .	22
1.3	Problem Statement . . . . .	23
1.4	Thesis Outline . . . . .	23
<b>2</b>	<b>Prototypes</b>	<b>24</b>
2.1	Initial Prototype . . . . .	24
2.2	OmniCopter . . . . .	26
2.2.1	Rotor Layout . . . . .	28
2.2.2	Variable Speed vs. Variable Pitch . . . . .	29
2.2.3	Redundant Torque Control . . . . .	30
2.2.4	Equations of Motion . . . . .	31
2.2.5	OmniCopter Prototype . . . . .	32
2.3	Requirements of Larger Overall Project . . . . .	34
2.3.1	Inclement Weather . . . . .	34
2.3.2	Localization . . . . .	34
2.3.3	Asymmetric Loading . . . . .	35
2.3.4	Management of Umbilical Cable . . . . .	35
2.3.5	Failure Modes . . . . .	35
2.3.5.1	Collisions . . . . .	35
2.3.5.2	Rotor Failures . . . . .	35
2.3.5.3	Flight Control System . . . . .	36
<b>3</b>	<b>Control Implementation</b>	<b>37</b>
3.1	Overview . . . . .	37
3.2	BlackTrax Motion Capture System . . . . .	38
3.2.1	Advantages over Unmodified Motion Capture System . . . . .	43
3.3	Control PC . . . . .	44

3.4	Control System Algorithm . . . . .	44
3.5	Serial PPM Converter and RC Transmitter Module . . . . .	48
3.6	UAVs . . . . .	50
<b>4</b>	<b>Testing, Results, and Discussion</b>	<b>53</b>
4.1	Rotor Tests . . . . .	53
4.1.1	Rotor Testing Setup . . . . .	54
4.1.2	Validating Thrust Model . . . . .	54
4.1.3	Thrust Rates . . . . .	56
4.2	Initial Flight Testing . . . . .	57
4.3	Disturbance Rejection . . . . .	59
4.3.1	Station Keeping Benchmark Tests . . . . .	59
4.3.2	Station Keeping in Gusting Winds . . . . .	63
4.4	Landing on an Inclined Surface . . . . .	65
4.5	Velocity Matching . . . . .	68
<b>5</b>	<b>Conclusions and Recommendations for Future Work</b>	<b>73</b>
5.1	Recommendations Future Work . . . . .	75

# List of Tables

2.1 Specifications for the OmniCopter prototype. . . . .	33
--	----

# List of Figures

1.1	Overview of the AMS project [5]. . . . .	3
1.2	Aircraft classification based on flying principle and propulsion mode [7]. . . . .	6
1.3	Hexrotor with 2-DOF manipulator carrying a payload [20]. . . . .	10
1.4	Large multirotor with 7-DOF manipulator [21]. . . . .	11
1.5	Shrouded rotor for increased efficiency [24]. . . . .	12
1.6	Sprung rotor mount for management of blade-flapping dynamics. [25]. . . . .	13
1.7	Large eddy simulation [26]. . . . .	14
1.8	Prototype demonstration of a passively-activated grasping foot for perching [29]. . . . .	15
1.9	Quadrotor with an additional perpendicular actuator to apply force to a wall [34]. . . . .	18
1.10	Dexterous hexrotor with fixed-pitch rotors [32]. . . . .	19
1.11	Variable-pitch hexrotor [35]. . . . .	19
1.12	Novel UAV with 5 rotors [36]. . . . .	20
1.13	Novel UAV with 5 rotors [37]. . . . .	21
1.14	Fully omni-directional UAV with 8 rotors [38]. . . . .	22
2.1	Top view of initial prototype with 3D-printed propeller guards. . . . .	25
2.2	3D-printed landing gear and propeller guards of initial prototype. . . . .	26
2.3	Rotor Layouts . . . . .	29
2.4	Layout 4. . . . .	29

2.5	Layout 5.	30
2.6	Definition of OmniCopter body-frame and rotor numbering.	31
2.7	OmniCopter prototype.	33
3.1	Overview of Control Implementation.	39
3.2	Location of position markers on UAVs.	40
3.3	Motion capture testing area [5].	40
3.4	Two Optitrack USB cameras mounted on a telescopic tripod.	41
3.5	BlackTrax Timekeeper and beacons. One beacon is shown removed from its casing for weight reduction, with high-gauge wire soldered directly to the PCB.	41
3.6	Representation of BlackTrax Motion Tracking System.	42
3.7	Diagram of Control PC functions.	45
3.8	Control for roll, pitch, and yaw.	47
3.9	Control for X and Y position.	47
3.10	Control for Z position.	47
3.11	RC Transmitter with modification to allow external PPM signal input.	49
3.12	Electrical schematic of Serial PPM Converter.	49
3.13	Block diagram describing the UAVs.	51
4.1	An orthogonal thrust rotor mounted on the thrust stand for testing.	55
4.2	Thrust vs. RPM plots.	55
4.3	Thrust vs. ESC input signal plots.	56
4.4	Test for orthogonal thruster maximum rates of change.	57
4.5	The OmniCopter hovering while maintaining a constant roll angle.	58
4.6	Control using the traditional roll/pitch control method.	60
4.7	Control using the orthogonal thruster control method.	61
4.8	Enlarged sections of station keeping in calm conditions comparison test.	62

4.9	A large fan used to simulate gusting winds. . . . .	64
4.10	Station keeping in simulated gusting wind. . . . .	66
4.11	A action-sequence of the OmniCopter landing on an inclined surface (20 degrees incline). . . . .	67
4.12	An action-sequence of the OmniCopter landing on an inclined surface (30 degrees incline). . . . .	68
4.13	An action-sequence of the OmniCopter matching the position and ve- locity of a ground vehicle. . . . .	69
4.14	An action-sequence of the OmniCopter matching a moving goal position. . . . .	70
4.15	Matching a moving goal position. . . . .	72

# Glossary

**AAV** Autonomous Aerial Vehicle.

**AMS** Aerial Manipulator System.

**CoG** Centre of Gravity.

**DOF** degree-of-freedom.

**ESC** Electronic Speed Controller.

**IMU** Inertial Measurement Unit.

**IR** Infrared.

**MAV** Micro Aerial Vehicle.

**MCU** Microcontroller Unit.

**MEMS** Micro-Electro-Mechanical-Systems.

**MTOW** Mean Take Off Weight.

**PID** Proportional-Integral-Derivative.

**PPM** Pulse Position Modulation.

**PWM** Pulse Width Modulation.

**RC** Remote Control.

**ROS** Robot Operating System.

**RPA** Remotely Piloted Aircraft.

**RPAS** Remotely Piloted Aircraft System.

**RPV** Remotely Piloted Vehicle.

**UAS** Unmanned Aircraft System.

**UAV** Unmanned Aerial Vehicle.

**VTOL** Vertical Take Off and Landing.



# Chapter 1

## Introduction

The aim of technological advancement has always been to expand the sphere of human influence. Through the development of technology, in a very general sense, we strive to increase our ability to affect change in the world.

The field of robotics typically does this for tasks which are repetitive, hazardous, or require a high degree of precision. Originally, robotics was predominated by robotic arms, called mechanical manipulators. Manipulators served as a general-purpose automation tool. A manipulator can exert forces or position objects anywhere within its reach. This, combined with its programmability, creates a flexibility which makes it very appealing as a solution to automation tasks. Applications of manipulators include automated welding, material handling, and assembly [1]. As is usually the case with automation, robot manipulators are faster, cheaper, and more accurate than humans are at performing the same tasks.

Mobile robotics extends the reach of robotics both figuratively and literally. For example, by mounting a manipulator on a mobile base the workspace of a manipulator is extended to anywhere the base can travel to. This broadens the applications of

robotics to include tasks in hazardous, hard to get to, or inhospitable environments. Examples of such environments include in space, undersea, in highly radioactive environments, and in mines and other underground locations. Mobile robotics includes more than just the transportation of manipulators, however. Applications include everything from inventory management in warehouses, automated vacuuming and lawn mowing, search and rescue, bomb defusal, and surveillance.

In general, the purpose of mobile robotics is to bring our technology to the places mankind wants and needs it. It is precisely this niche which is the focus of this thesis, that served by UAVs.

## 1.1 Background

The term UAV refers to a flying machine without the presence of an on-board pilot or passengers [2]. It may be either piloted remotely (remote control) or via on-board processes (autonomously), or some combination thereof with various degrees of human involvement and supervision. The qualifier *reusable* is used in some definitions to distinguish UAVs from guided weapons like cruise missiles. A variety of other terms are used, including Unmanned Aircraft System (UAS), Remotely Piloted Vehicle (RPV), Remotely Piloted Aircraft (RPA), Remotely Piloted Aircraft System (RPAS), Micro Aerial Vehicle (MAV), and Autonomous Aerial Vehicle (AAV). The most commonly recognized term used by the general public is ‘drone’ which is what the remote controlled aircraft used by the U.S. Navy for target practice were originally called [3].

This thesis focuses on one component of a larger project in which an Aerial Manipulator System (AMS) is to be developed. This project, described in detail in [4] and [5], requires an aerial platform capable of proximity flying and landing on structures. A

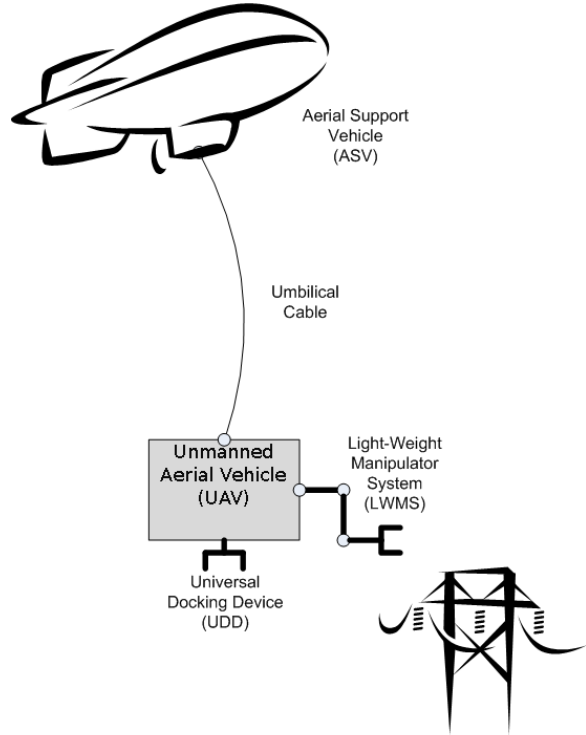


Figure 1.1: Overview of the AMS project [5].

diagram providing a conceptual overview of the larger project is shown in Figure 1.1. The goal of the greater project is to develop a system capable of application in very remote areas for inspection, construction, and/or maintenance of infrastructure such as power transmission lines, oil pipelines, or other similar structures. In the system proposed for this, a large lifting-gas ‘mothership’ will autonomously travel along the pipeline or power transmission line. The ‘mothership’ will supply power via a physical cable, denoted ‘Umbilical Cable’ in Figure 1.1, to a smaller autonomous aerial vehicle which will conduct the actual inspection or servicing task. This thesis focuses on the development of the smaller UAV at the end of the physical cable.

## 1.2 Literature Survey

### 1.2.1 Overview

The literature survey is broken into eight sections, each of which covers an area of research related to the thesis topic and summarizes several key papers and their most relevant points.

The first section covers the classification of UAVs and defines quadrotors and multirotors. The next section covers work which focuses on inspection and other forms of data collection by UAVs. The following section covers control strategies for UAVs as well as control challenges related to UAVs which perform perching, grasping, or aerial manipulation tasks. The Vehicle Aerodynamics section covers work related to UAV vehicle aerodynamics while the section on Environmental Aerodynamics covers challenges associated with aerodynamics of the environments in which UAVs operate. The section titled Grasping and Perching covers work related to UAVs grasping objects for transportation or grasping features for maintaining a secure landing position. The section titled Aerial Manipulation covers work related to aerial manipulators and the associated control challenges. The final section titled Novel UAV Platforms describes several novel UAV designs which aim to improve on existing traditional multirotors for aerial manipulation tasks.

### 1.2.2 Classification of UAVs

Several different methods exist to classify UAVs in order to differentiate existing systems and their operational capabilities as well as to provide a regulatory framework which helps determine the degree of risk associated with UAVs [6]. Five systems of categorization are described:

- Classification based on Mean Take Off Weight (MTOW) and Ground Impact

### Risk

- Classification based on Operational Altitude and Midair Collision Risk
- Classification based on Autonomy
- Military Classifications
- Classification based on Ownership

Figure 1.2 depicts another classification scheme from [7] in which UAVs are categorized based on principle of flight and propulsion mode. It should be noted that while the figure correctly classifies quadrotors as motorized Vertical Take Off and Landing (VTOL) UAVs, this category can be generalized to traditional multirotors. Traditional quadrotors use four fixed-pitch co-planar rotors to generate lift. Two rotors rotate clockwise and two rotors rotate counterclockwise. Traditional multirotors simply add counter-rotating redundant pairs of rotors to a quadrotor concept.

The remainder of the literature survey will focus primarily on work pertaining to traditional multirotors and applications pertaining to aerial mobile manipulators as this is the intended type of vehicle which will be used in the larger AMS project.

### 1.2.3 Aerial Inspection

Aerial inspection or, in general, data collection and observation tasks, are in many ways much easier for UAVs than any task which requires physical interaction with the environment. The UAV can maintain a greater distance from surrounding objects and does not need to come into physical contact with them. This means the need for precise control can be somewhat relaxed compared to aerial manipulator systems. Many commercial UAV applications already exist, including:

- Aerial video and photography
- Crop dusting

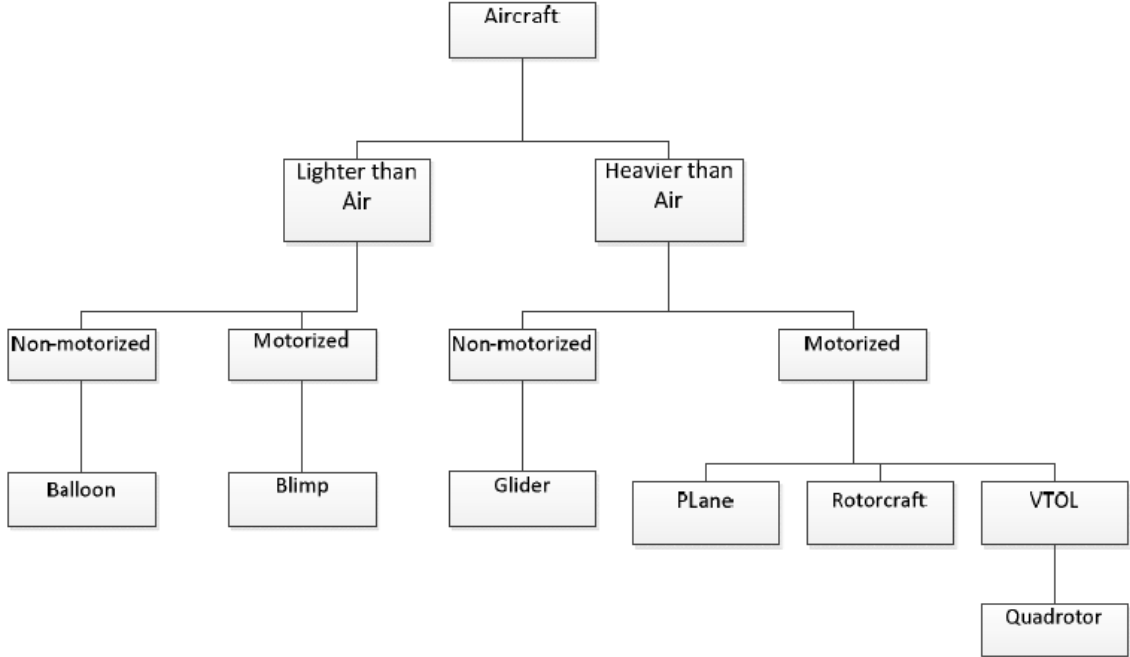


Figure 1.2: Aircraft classification based on flying principle and propulsion mode [7].

- Search and rescue
- Construction surveying
- Mining
- Traffic surveillance

In [8], an assessment of the quality of UAV-based visual inspection of structures is given. The influence of parameters such as lighting conditions, distance from objects, and vehicle motion on the quality of visual data such as photographs and videos is studied. In particular, the effect of fluctuating wind speed and wind direction is examined. An important concept is the idea that while constant wind speeds can be reliably corrected for, fluctuations in wind speed and direction cause time-varying aerodynamic forces on UAVs which cause vehicle motion due to correction lag. Additionally, fluctuations generated by local aerodynamics around the structure can be significant. Methods are developed to automatically detect the harmful effects of such motions by examining the images.

In [9], the use of UAVs to inspect high voltage power lines is considered. A system is developed in which a quadrotor is equipped with a visual spectrum camera and a thermal-infrared camera. Using these two sensors to record data and flying under the control of a human operator, inspections of high voltage power lines are carried out and several common types of faults are detected.

#### 1.2.4 UAV Modelling and Control

A derivation of quadrotor dynamics is presented in [10]. By assuming that motor resistance is negligible and that no-load motor current is small, the force generated by one motor is approximated as proportional to the square of the angular velocity of the rotor. The total force,  $\mathbf{F}_B$ , generated in the body frame of the quadrotor is then given as:

$$\mathbf{F}_B = k \begin{bmatrix} 0 \\ 0 \\ \sum_{i=1}^4 \omega_i^2 \end{bmatrix} \quad (1.1)$$

where  $\omega_i$  is the angular velocity of the  $i^{th}$  rotor and  $k$  is a proportionality constant which accounts for properties of the motor and propeller.

A global drag force,  $\mathbf{F}_D$ , is modelled, proportional to velocity in the Cartesian coordinates as:

$$\mathbf{F}_D = \begin{bmatrix} -k_d \dot{x} \\ -k_d \dot{y} \\ -k_d \dot{z} \end{bmatrix} \quad (1.2)$$

where  $k_D$  is the drag coefficient and  $\dot{x}$ ,  $\dot{y}$ , and  $\dot{z}$  are the translational velocities in the X, Y, and Z directions, respectively.

By neglecting the component due to angular acceleration of the rotor, the torque,  $\tau_z$ , generated by a rotor about the Z axis is given as:

$$\tau_z = b\omega^2 \quad (1.3)$$

where  $b$  is a proportionality constant which accounts for the properties of the motors and propellers as they relate to torque and  $\omega$  is the angular velocity of the rotor. The total torque experienced by the quadrotor in the body frame about its Z axis,  $\tau_\psi$ , is given as:

$$\tau_\psi = b(\omega_1^2 - \omega_2^2 + \omega_3^2 - \omega_4^2) \quad (1.4)$$

where  $\omega_i$ ,  $i = 1$  to 4, are the four rotor velocities.

Note that the positive rotation directions for the rotors are defined such that a positive rotation always results in an upwards force.

The torques about the roll ( $\tau_\phi$ ) and pitch ( $\tau_\theta$ ) axes in the quadrotor body frame are given as:

$$\tau_\phi = Lk(\omega_1^2 - \omega_3^2) \quad (1.5)$$

and

$$\tau_\theta = Lk(\omega_2^2 - \omega_4^2) \quad (1.6)$$

where  $L$  is the distance from the centre of mass to the centre of one rotor.

The total torque in the body frame,  $\tau_B$  is:

$$\boldsymbol{\tau}_B = \begin{bmatrix} Lk(\omega_1^2 - \omega_3^2) \\ Lk(\omega_2^2 - \omega_4^2) \\ b(\omega_1^2 - \omega_2^2 + \omega_3^2 - \omega_4^2) \end{bmatrix} \quad (1.7)$$

The resulting equations of motion are then:

$$m\ddot{\mathbf{x}} = \begin{bmatrix} 0 \\ 0 \\ -mg \end{bmatrix} + \mathbf{RF}_B + \mathbf{F}_D \quad (1.8)$$

where  $\mathbf{R}$  is a rotation matrix relating the body frame to the inertial frame,  $\ddot{\mathbf{x}}$  is the acceleration of the quadrotor,  $m$  is the mass, and  $g$  is the acceleration due to gravity. Of particular note is that the quadrotor is an under actuated system with four inputs and six outputs. Motion in the global reference frame is coupled with the orientation of the quadrotor body frame.

Many different control strategies have been applied to quadrotors including Proportional-Integral-Derivative (PID) [7,11–13], backstepping or neural networks [14–16], or other techniques and comparisons between different methods [14,17,18]. In [19] a concurrent learning adaptive controller is contrasted with PID control. The authors note that while PID control has been shown to yield excellent results, PID control requires time-intensive tuning of parameters and the resulting controllers and parameters are not easily transferable to other quadrotors. They successfully demonstrate using adaptive control to augment a controller transferred from another quadrotor whose inertial characteristics and throttle mapping are very different.

In [20], online parameter-estimation was used to compensate for an unknown payload.



Figure 1.3: Hexrotor with 2-DOF manipulator carrying a payload [20].

A payload with mass unknown to the controller is carried by a 2-degree-of-freedom (DOF) arm attached to a hexrotor, an example of which can be seen in Figure 1.3. The arm remained in a fixed orientation during the tests.

In [21] a 7-DOF arm was mounted underneath a multirotor and a backstepping-based controller that uses the coupled full dynamic model is compared to a PID controller. It is shown that the standard PID controller with no knowledge of the arm position or movement shows noticeable deflection of the pitch of the UAV during arm movement, while the backstepping-based controller shows no noticeable change in pitch deflection during arm motion, likely due to the controller's ability to account for the arm's dynamics. Figure 1.4 shows this UAV in flight with the manipulator extended.

One of the most significant works in UAV control is [22]. In this paper the authors show that quadrotor dynamics with four inputs, such as are presented at the beginning of this section, are *differentially flat*. As described in [23], “differential flatness provides an analytical mapping from a path and its derivatives to the states and con-



Figure 1.4: Large multirotor with 7-DOF manipulator [21].



Figure 1.5: Shrouded rotor for increased efficiency [24].

trol input required to follow that path. This powerful property effectively guarantees feasibility of any differentiable trajectory, provided that its derivatives are sufficiently bounded to avoid input saturation, thus eliminating the need for iterative simulation in the search for trajectories.” The work in [23] extends [22] to allow improved generation of trajectories for quadrotors.

### 1.2.5 Vehicle Aerodynamics

The advantages of shrouded rotors over unshrouded ones were examined in [24]. Under static hover conditions, a 15% net benefit in payload was demonstrated after accounting for the additional weight of the rotor shroud. Under edgewise flow conditions between 2-2.5 times greater drag and pitching moment was experienced by the shrouded rotor over the unshrouded rotor. Figure 1.5 depicts a rotor with a shroud such as was tested.

In [25], the authors attempt to increase thrust and manage unstable dynamic behaviour of a quadrotor by designing an optimized rotor and flexible propeller mount system. More specifically, the authors attempt to mitigate issues caused by rotor blade flapping by mounting the rotor blades to the rotor using torsional springs, as



Figure 1.6: Sprung rotor mount for management of blade-flapping dynamics. [25].

seen in Figure 1.6. To optimize thrust, an iterative simulator using MATLAB was used to find optimal rotor blade parameters. Physical rotors were tested and the thrust produced corresponded closely to the value predicted by the simulation.

### 1.2.6 Environmental Aerodynamics

A lengthy study of airflow patterns near large structures, such as would be found in urban environments, is presented in [26]. The purpose of this work is to understand potential challenges associated with operating fixed-wing UAVs at low altitude in a dense urban environment with large tall structures. A large variety of wind tunnel tests and simulations were conducted to explore the characteristics of air flow around large structures. Figure 1.7 shows an example of a simulation with two rectangular buildings. While the results show that air flows around large structures can be predicted, testing was only conducted to explore static conditions. The incident wind direction and velocity were held constant allowing steady state flow conditions to develop around the structures. In these conditions, large air velocity gradients were observed in the proximity of the structures, and large eddy fields were observed in the wake of the structures. Both of these factors could pose challenges for UAVs operating in proximity of the structures.

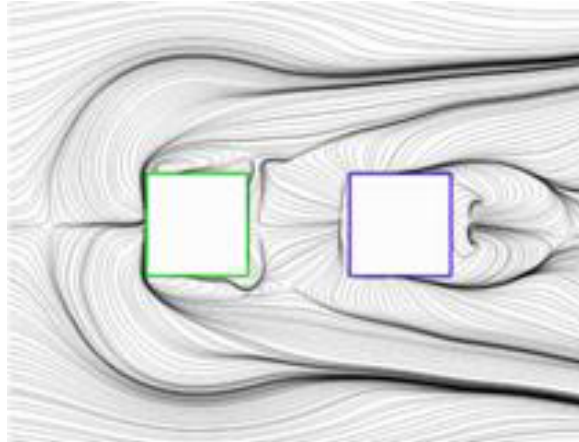


Figure 1.7: Large eddy simulation [26].

The problem of flying in proximity to the ground is addressed in a paper on aerial grasping [27]. The authors note that, "when flying close to the ground, rotor down-wash is contained by the surface underneath it creating a cushion of air referred to as 'ground effect.'"

Another approach to environmental aerodynamic effects on UAVs is taken in [28]. In this paper the authors attempt to model and map the aerodynamics in the environment in order to exploit them. The authors note that birds experience benefits such as improved flight efficiency, superior localization, better decision making, and survival as a result of aerodynamic effects caused by the environment. The effects of the proximity of large horizontal surfaces above and below a small quadrotor are measured. A model for ground effects was produced and used in a subsequent test. A quadrotor was flown in a grid pattern over several objects and a terrain map was produced based on the rotor speed of the UAV. The location of the objects could be seen clearly from the plot of rotor speed and position.



Figure 1.8: Prototype demonstration of a passively-activated grasping foot for perching [29].

### 1.2.7 Grasping and Perching

In [27], a scale Remote Control (RC) helicopter was outfitted with a compliant four-fingered gripper and experiments were conducted lifting a payloads of a variety of shapes and masses. A human pilot manually flew the helicopter to a position above the target payload, descended, and activated the gripper mechanism to pick up the target payload and take-off again. No autonomous compensation for offset loads was used. The authors note experiencing unexpected challenges with gusting winds while in hover close to the ground, including instances where landing skids came into contact with the ground causing the helicopter to tip over.

In [29] an avian-inspired passively actuated gripping mechanism was developed for VTOL UAVs. The design is intended to allow a UAV to land on long thin rod-like

features such as tree branches or power lines. Figure 1.8 shows the gripping mechanism being actuated by a downwards force applied to the top of the gripper’s ‘leg.’ The intention is that gravity acting on the mass of the vehicle provides this downwards force causing the gripping mechanism to be activated as the vehicle lands on a feature. The significant benefit of this approach is that no power is required to maintain a grip on a landing feature, allowing the vehicle to recharge or conserve power for other operations.

Several different light-weight low-complexity grippers were designed and tested in [13]. These grippers were used on small quadrotors to pick up payloads composed of deformable porous material such as wood, foam, or fabric. Parameter estimation was used to compensate for the presence of payloads, estimating the payload’s moments of inertia, mass, and position of the payload’s centre-of-gravity with respect to the UAV.

In [30], a subsequent work by the same authors, the grippers from [13] were used to allow multiple quadrotors to cooperatively grasp and transport payloads. This overcomes the limited payload capacity of a single UAV by using teams of UAVs to lift the larger payload.

In [31], a quadrotor is outfitted with downwards-facing ultrasonic range finders. These sensors are used to measure the orientation of a large flat oscillating surface beneath the UAV. Two human operators hold a large flat sheet of wood and manually tilt it back and forth while the UAV hovers above this surface between them. The UAV matches the orientation of the oscillating surface in order to allow it to land on it as it oscillates. The authors note that at low oscillation frequencies the UAV tended to drift away from the landing platform due to the inherent property of moving in the direction of the tilt.

### 1.2.8 Aerial Manipulation

Several important concepts for aerial mobile manipulator systems are highlighted in [32]. First and foremost is the importance of *force closure* for manipulators. Force closure is defined as the ability of a mechanism to directly resist any arbitrary wrench, or combination of force and torque. This is an important property for dexterous manipulators. A mobile manipulator base must have force closure because forces exerted by a manipulator are transferred to the base. This is not a major issue for ground-based mobile manipulators due to contact with the ground providing frictional resistance to forces. Aerial manipulator bases cannot depend on friction with the environment to allow them to resist forces and torques.

Several important observations about traditional multicopters are also made. Since all rotors on traditional multicopters face in a parallel direction, they can only generate forces along this axis. If one designates this direction the Z axis, then it can be said that generating linear forces along X and Y is impossible for a traditional multicopter. Traditional multicopters can only pitch, roll and yaw and lift. In order to move in the X and Y directions a traditional multicopter must first pitch or roll. This means that these systems are nonholonomic. The same holds true for helicopters. These characteristics make traditional multicopters and helicopters unsuitable for mobile manipulation.

Challenges arising from using nonholonomic bases for mobile manipulators are noted in [33]. In this paper a 6-DOF manipulator for aerial mobile manipulation tasks was developed. The authors note that for rotary wing UAVs, reaction torques caused by changes in the position of the the manipulator's Centre of Gravity (CoG) produce an inclination of the rotor's plane which also induces a displacement of the entire aerial platform. This is due to the coupled nature of orientation with translational motion

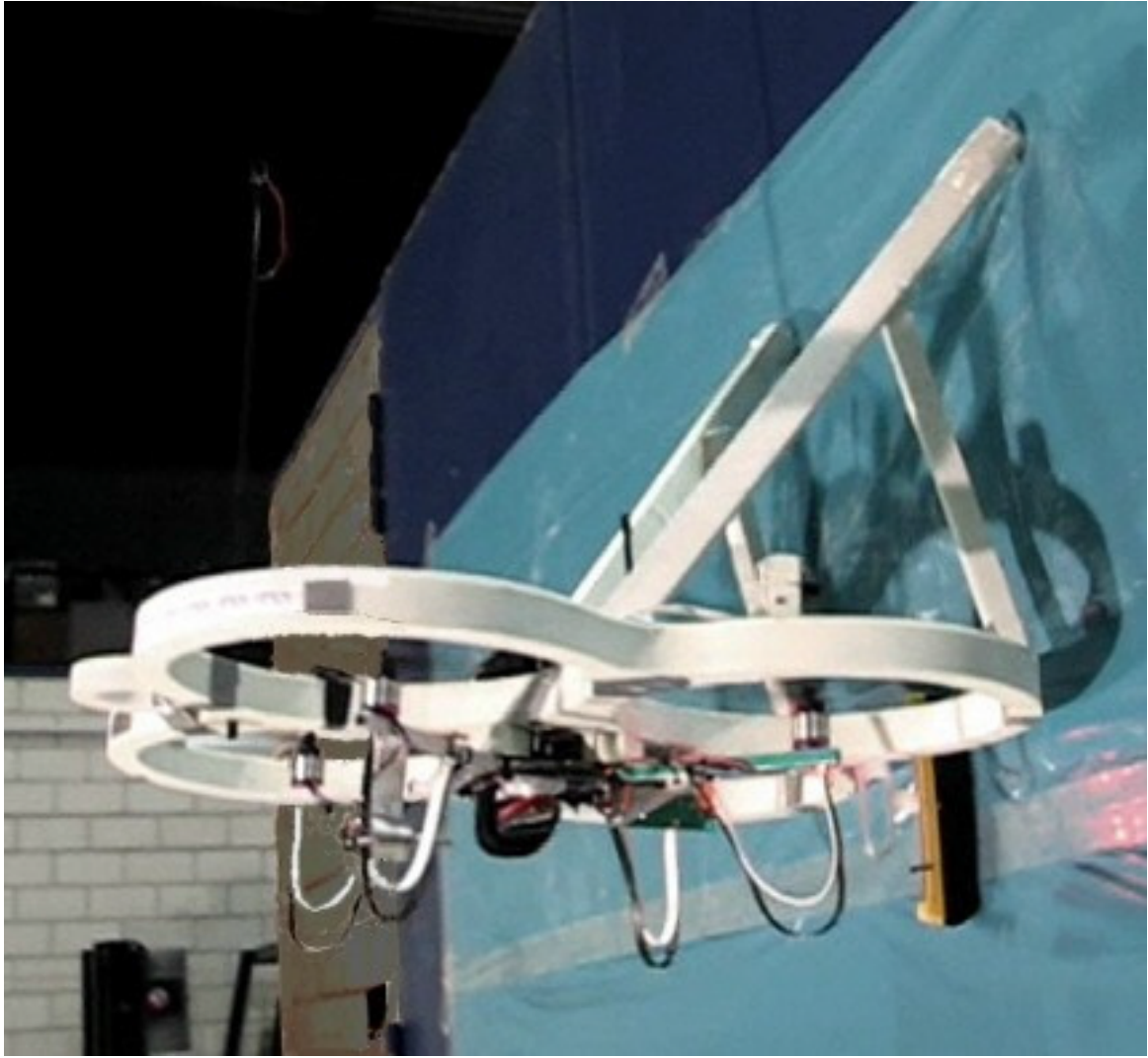


Figure 1.9: Quadrotor with an additional perpendicular actuator to apply force to a wall [34].

for traditional multicopters and helicopters.

### 1.2.9 Novel UAV Platforms

In [34], a single actuator was added to a traditional quadrotor design to allow their UAV to apply a horizontal force to vertical surfaces while in flight, as seen in Figure 1.9. This is used to facilitate tasks such as cleaning walls or windows.

In order to overcome the limitations of traditional multirotors and helicopters, a novel hexrotor design was developed in [32]. In order to generate off-axis forces, the rotors'

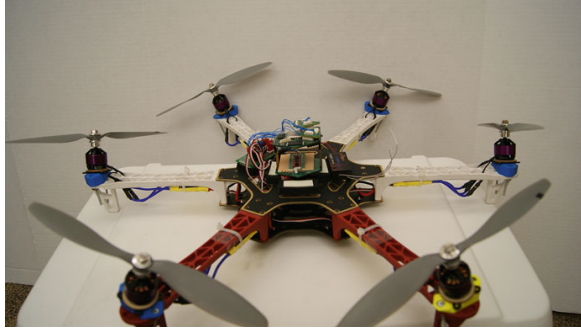


Figure 1.10: Dexterous hexrotor with fixed-pitch rotors [32].

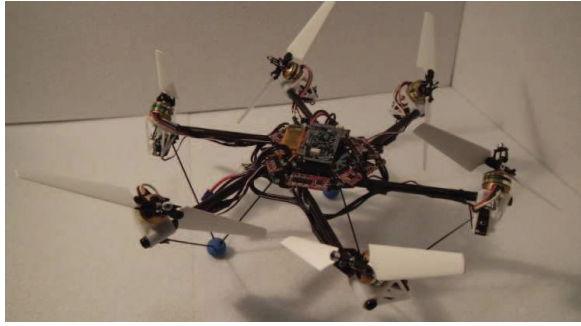


Figure 1.11: Variable-pitch hexrotor [35].

axes of thrust are canted by 30 degrees such that they are no longer parallel, as pictured in Figure 1.10. This is very similar to [35] except that in [35] the rotors are canted at 45 degrees and variable pitch rotors are used as opposed to variable speed ones, as pictured in Figure 1.11. In [35], the authors indicate that the primary benefit is the ability to fly in arbitrary body attitudes.

In [36], a UAV with five rotors was developed and constructed. The large central rotor, as seen in Figure 1.12, is responsible for generating the majority of the lift while the three outer rotors are used for maneuvering. The three outer rotors can rotate into a configuration where their axes of thrust are perpendicular to the main lift rotor. In this work, simulations of circular path tracking were conducted and the authors note that the UAV is capable of tracking the circular path while maintaining zero attitude orientation. The authors note that quadrotors are limited due to being

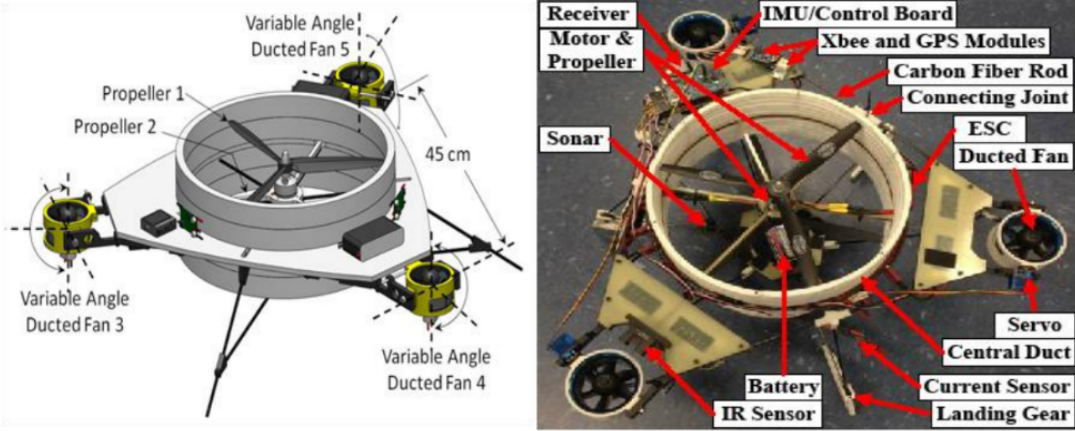


Figure 1.12: Novel UAV with 5 rotors [36].

underactuated, that a sensor or gripper could not be arbitrarily oriented during flight, and that a quadrotor cannot hover in place with any body orientation.

In [37], an eight rotor UAV was developed with four rotors added outwards of a standard quadrotor design. The additional four rotors are facing perpendicular to the original four quadrotor rotors as shown in Figure 1.13. The resulting UAV has translational and rotational dynamics almost completely decoupled, with the exception being that there is some aerodynamic interaction between the rotors due to the fact that the horizontally facing rotors direct an airstream directly underneath the lifting rotors.

In [38], a fully omni-directional UAV with eight rotors is presented. The geometric configuration of rotors was chosen to maximize agility in any direction. Testing on a prototype vehicle demonstrated an ability to rotate about an axis independently of translational movement. The rotations were performed while maintaining a hover position with an error between 5 and 10 cm. In another test, the UAV was commanded to track a circle of 1.5 m at 1.95 m/s, and was able to maintain a position accuracy between 10 and 15 cm. In this test the results indicated a coupling between



Figure 1.13: Novel UAV with 5 rotors [37].

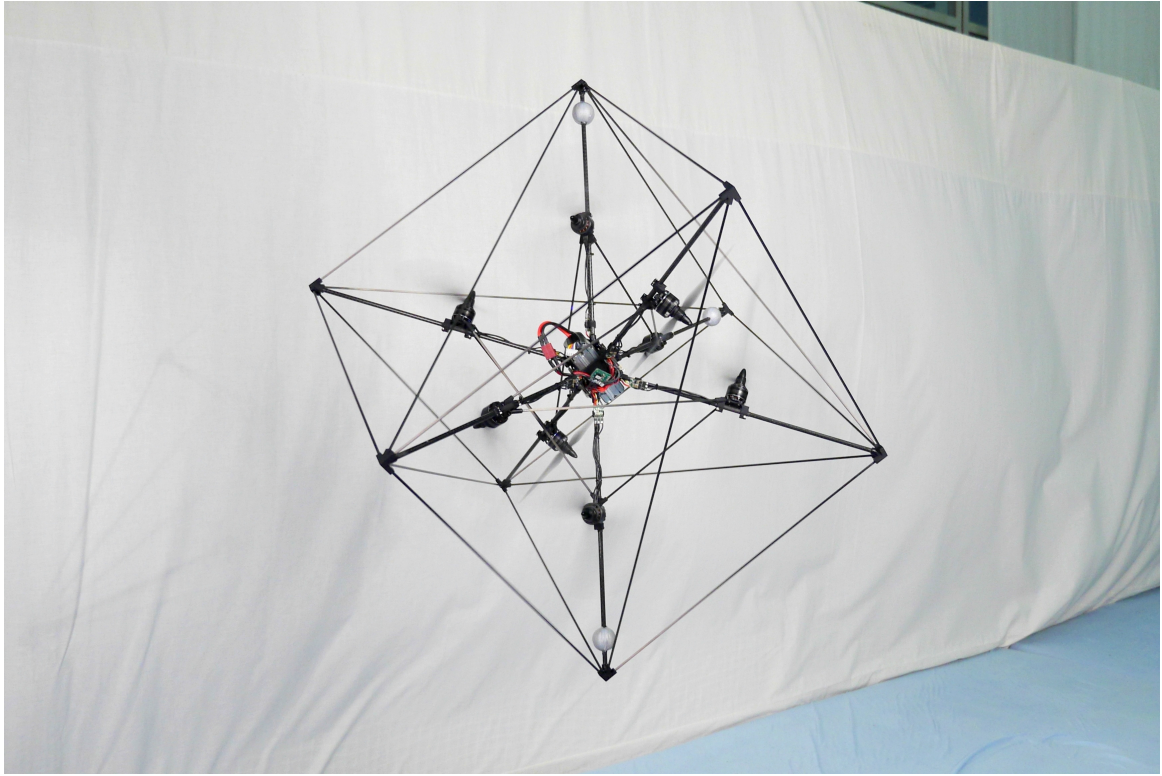


Figure 1.14: Fully omni-directional UAV with 8 rotors [38].

translational and rotational dynamics, potentially due to unmodelled aerodynamic interactions between rotors.

### 1.2.10 Summary

Three main themes can be identified from the literature as it pertains to aerial mobile manipulators.

1. Unpredictable aerodynamic forces create challenges for UAVs operating near the ground or in proximity to large structures.
2. Aerial mobile manipulator bases must actively manage forces resulting from physical contact with the environment during perching, grasping, manipulation, and transportation of payloads.
3. Traditional multicopters and helicopters have significant limitations due to their

nonholonomic or under actuated nature.

### 1.3 Problem Statement

The objective of this thesis is to develop an autonomous aerial mobile base capable of positioning a manipulator arm such that the system can ultimately perform inspection, construction, and/or maintenance tasks. All electrical power requirements are to be satisfied through a physical cable, relieving flight-time, thrust capacity, and payload capacity considerations. The UAV should satisfy the following requirements:

- Accurately control pose in the presence of unpredictable aerodynamic forces.
- Support the future use of a docking device to land or perch on industrial structures.
- Handle forces resulting from physical contact with the environment during landing, docking, manipulation tasks, and transportation of payloads.

### 1.4 Thesis Outline

The remaining outline of the thesis is as follows. Chapter 2 presents a description of two prototypes built for this work. The first of these prototypes was used during the development of the hardware and software of the control system. The second prototype is a prototype of a novel multirotor UAV. Chapter 3 describes the hardware and software components of the control system in detail. Chapter 4 describes the tests that were conducted, the results that were obtained, and a discussion on their significance. Chapter 5 summarizes the findings and presents some recommendations for future work.

# Chapter 2

## Prototypes

### 2.1 Initial Prototype

A small UAV prototype was initially constructed as a first step so that the broader UAV testing system could be developed. The control system is composed of components which are required to control the UAV during development and testing but which are not part of the UAV itself. The control system is described in further detail in Chapter 3.

The initial prototype was based on an off-the-shelf quadrotor HobbyKing FPV250 kit. A set of modular 3D-printed propeller guards was added for safety and to prevent frequent propeller breakage during the initial development stage. This is shown in Figure 2.1. Flexible landing gear were also added to prevent damage during landings and can be seen in Figure 2.2. This prototype measured 250 mm diagonally from rotor centre to rotor centre and used a 79 gram, 1,000 mAh, 11.1 V Lithium-Polymer battery for power.

Numerous test flights were conducted with the initial prototype, providing invaluable



Figure 2.1: Top view of initial prototype with 3D-printed propeller guards.



Figure 2.2: 3D-printed landing gear and propeller guards of initial prototype.

experience and insight into the challenge of autonomous control for multirotors. Initially, PID control was attempted to adjust roll or pitch angle based on the error in position and the setpoint. This approach did not work very well and led to using PID control to attempt to match a desired velocity, rather than operating on the error in position. Better performance with this method was observed and this is the method used for control of the second prototype, the OmniCopter.

## 2.2 OmniCopter

In the following section, the development of a UAV concept and prototype which satisfies the criteria laid out in the problem statement is presented.

In order to maintain a desired vehicle pose in the presence of unpredictable aerodynamic forces the UAV must have good disturbance rejection. This property is

determined by the vehicle dynamics as well as the characteristics of the actuators, sensors, and control algorithm. Primarily, the UAV needs to be capable of reacting *promptly* to disturbances. A traditional multicopter lacks the ability to respond to a lateral force promptly because it is delayed by the time it takes to tilt in order to generate a compensating lateral force.

Here some principles from Axiomatic Design [39] may be applied. If one considers translational movement and adjusting orientation to be separate requirements, as they are for mobile aerial manipulators, then the independence axiom requires that these remain independent. Thus, by decoupling control of orientation from control of translation one can satisfy the independence axiom. To do this, the addition of laterally directed rotors is proposed. This would make the UAV omni-directional and, as such, address the other two criteria as well. A docking mechanism can be easily positioned relative to a landing feature if the vehicle's orientation is independent of its translational motion. Similarly, if a torque induced by an off-centre payload causes rotation, this will not necessarily result in translational motion.

In [32], a strong case for the necessity of force closure in aerial mobile manipulator bases is made. As defined in [40], force closure is the ability of a mechanism to directly resist any arbitrary wrench applied to it. As noted in [32], the inability of a mobile base to resist arbitrary wrenches means the manipulator also cannot resist arbitrary wrenches, and as such cannot effectively perform manipulation tasks. In higher friction environments or with heavy mobile bases this issue may be ignored without serious consequences. However, for aerial manipulator bases, force closure becomes very important. The OmniCopter can resist any combination of force and torque, meaning it has force closure.

Because sufficient power to the UAV is supplied by an external power source through a cable, concerns about the decrease in flight-efficiency and extra weight due to additional rotors can be dismissed.

### 2.2.1 Rotor Layout

Several rotor layouts were considered. Figure 2.3(a) shows a top view of a relatively straightforward approach whereby four additional rotors with thrust axes directed orthogonal to the main-lifting rotors are added. The additional rotors in Layout 1 are in-line with the main lift rotors and are outwards of the main body of the quadrotor. Their axes of thrust pass through, or very close to, the CoG of the UAV. Figure 2.3(b) shows a similar approach except that the additional orthogonal-thrust rotors are contained internally in the space between the main lift rotors, and are not in-line with the main cross-members of the frame. Their axes of thrust also pass through the CoG of the UAV. Figure 2.3(c) shows multi-view drawings of a rotor layout which contains 12 rotors and is essentially composed of three quadrotors bisecting each other in the X-Y, Z-X, and Z-Y planes. Figure 2.4 shows a layout with four thrust rotors arranged in diagonally offset pairs. Figure 2.5 shows a layout with only 6 rotors arranged in co-axial pairs on the X, Y, and Z axes.

Layouts 3-5 were not selected due to their excessive mechanical complexity and the limited space in which accessories such as manipulators, docking mechanisms, and data-collection sensors could be mounted. It was predicted that Layout 1 would experience detrimental aerodynamic interactions between the additional thrust rotors and the main lift rotors. If the thrust rotors were activated they would move air directly above and beneath the main lift rotors, thus reducing their effectiveness and changing the amount of lift created depending on whether the thrust rotors are in use. This creates an additional control challenge. In comparison to Layout 2, Layout

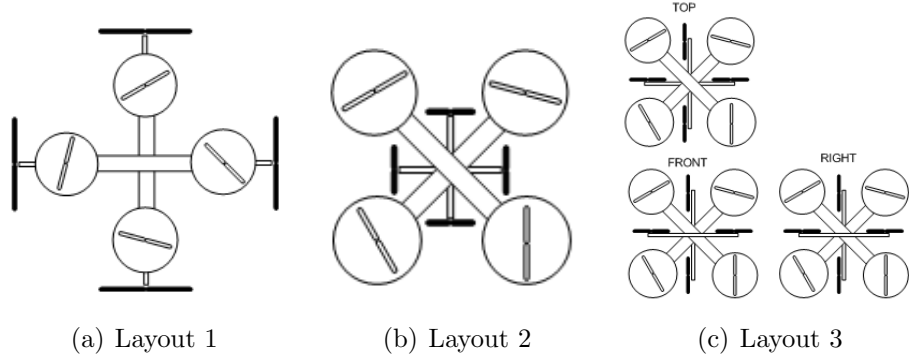


Figure 2.3: Rotor Layouts

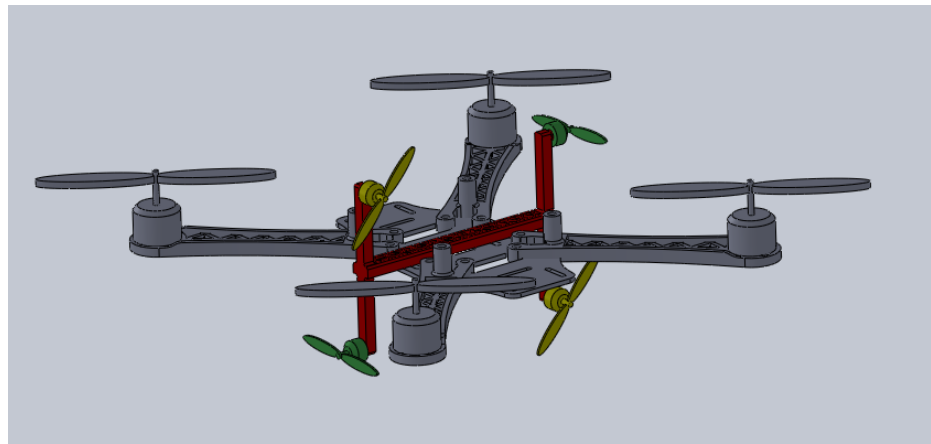


Figure 2.4: Layout 4.

1 is less space-efficient limiting how closely it can approach structures. Layout 2 was ultimately selected for further development, and is hereafter referred to as the OmniCopter.

### 2.2.2 Variable Speed vs. Variable Pitch

The OmniCopter uses variable speed rotors, and can reverse the direction of rotor rotation to reverse the direction of thrust. A variable pitch rotor would use a mechanism to adjust the pitch of the rotor blades in order to control the magnitude of thrust, while keeping rotor speed at a maximum. Variable pitch rotors can change the magnitude of thrust more quickly than variable speed rotors, whereas variable speed rotors are mechanically simpler, cheaper, lighter, easier to maintain, and more

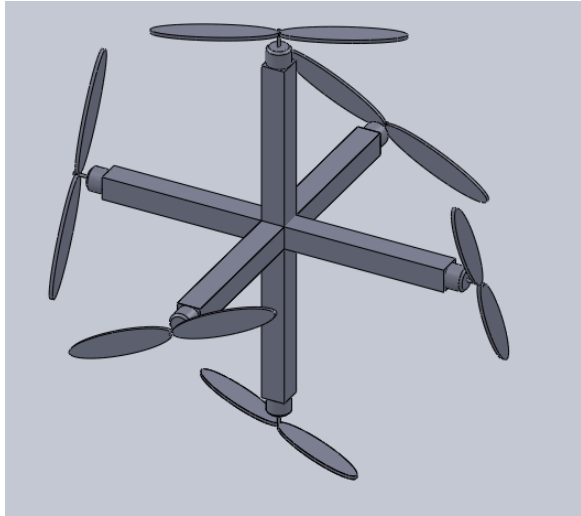


Figure 2.5: Layout 5.

reliable.

### 2.2.3 Redundant Torque Control

Each co-axial pair of thrust rotors is counter-rotating, and contains one clock-wise oriented propeller and one counter-clockwise oriented propeller. This was done so that the torque generated by the rotation of one rotor can be counteracted by the other rotor of that rotor pair. Since the propellers have opposite orientations, thrust is generated in the same direction while the rotors spin in opposite directions. A torque can be generated if the rotors spin in the same direction, while a net-zero thrust is generated. The sum of rotation rates determines net torque while the difference in rotation rates determines net thrust. Combinations of rotor speeds can be selected in order to generate desired combinations of torque and thrust.

Since the main lift rotors can be used to generate torques about all three axes independently, the addition of the thrust rotors gives the OmniCopter redundant control of torque for the roll and pitch axes. This means it could tolerate failure of some of the rotors.

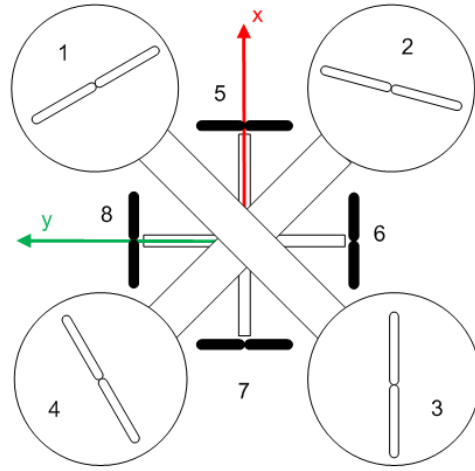


Figure 2.6: Definition of OmniCopter body-frame and rotor numbering.

## 2.2.4 Equations of Motion

The following section, which details the equations of motion of the OmniCopter, was developed by augmenting the equations of motion of a quadrotor, developed in [10], to include the additional rotors.

By defining the body-frame co-ordinate system and rotor numbering as shown in Figure 2.6, the torque in the body frame is given as:

$$\boldsymbol{\tau}_B = \mathbf{R}_Z(45^\circ) \begin{bmatrix} Lk(\omega_1^2 - \omega_3^2) \\ Lk(\omega_2^2 - \omega_4^2) \\ b(\omega_1^2 - \omega_2^2 + \omega_3^2 - \omega_4^2) \end{bmatrix} + \begin{bmatrix} k_t(\omega_5^2 + \omega_7^2) \\ k_t(\omega_6^2 + \omega_8^2) \\ 0 \end{bmatrix} \quad (2.1)$$

where  $\mathbf{R}_Z$  rotates the original body-torque matrix used from [10] about the Z axis to align it with the coordinate system shown in Figure 2.6, and  $k$  and  $k_t$  are constants of proportionality accounting for motor and propeller properties for the main rotors and orthogonal thrust rotors respectively.  $L$  is the distance from the centre of mass to the centre of one rotor, and  $b$  is a proportionality constant which accounts for the properties of the motors and propellers as they relate to torque. The forces developed

in the body-frame are given as:

$$\mathbf{F}_B = \begin{bmatrix} k_f(\omega_6^2 + \omega_8^2) \\ k_f(\omega_5^2 + \omega_7^2) \\ k \sum_{i=1}^4 \omega_i^2 \end{bmatrix} \quad (2.2)$$

and a drag force proportional to the vehicle's air velocity is given as:

$$\mathbf{F}_D = \begin{bmatrix} -k_d \dot{x} \\ -k_d \dot{y} \\ -k_d \dot{z} \end{bmatrix} \quad (2.3)$$

The equations of motion are:

$$m\ddot{\mathbf{x}} = \begin{bmatrix} 0 \\ 0 \\ -mg \end{bmatrix} + \mathbf{R}\mathbf{F}_B + \mathbf{F}_D \quad (2.4)$$

where  $\mathbf{R}$  is a rotation matrix relating the body frame to the inertial frame.

### 2.2.5 OmniCopter Prototype

A physical prototype, shown in Figure 2.7, was constructed and tests were conducted to determine the suitability of such a rotor layout as a base for an aerial mobile manipulator platform.

Specifications for the prototype are presented in Table 2.1.

A 2 meter long dual-conductor 14 AWG stranded copper cable was used to supply power from the battery to the prototype. The battery rested on the ground near the flight operating area.

Table 2.1: Specifications for the OmniCopter prototype.

Prototype Specifications	
Mass	1,513 grams
Frame diameter	620 mm
Main rotor diameter	11 inches
Main rotor pitch	4.5 inches
Maximum lifting thrust	3.7 kgF
Thrust rotor diameter	6 inches
Thrust rotor pitch	4.5 inches
Maximum horizontal thrust	1.0 kgF
Power source	Lithium-Polymer battery
Battery voltage	14.8 V
Battery capacity	10,000 mAh



Figure 2.7: OmniCopter prototype.

## 2.3 Requirements of Larger Overall Project

Although the requirements given in Section 1.3 cover the general needs of a tethered aerial manipulator base, some more consideration needs to be given to the specific requirements of such a UAV in the scope of the larger AMS project.

### 2.3.1 Inclement Weather

The AMS must be able to operate in or withstand all but the most extreme weather conditions due to operating in remote areas without human supervision. As such, it must be designed to withstand the following:

- Precipitation
- Fog
- Cold
- Heat
- Heavy wind

Although flight and operation in windy conditions must be possible, a method of mooring, sheltering, or otherwise sustaining conditions when winds exceed certain limits must also be planned for.

### 2.3.2 Localization

Both the lifting-gas support vehicle and the smaller aerial manipulator base UAV must carry their own on-board localization systems. These localization systems should use multiple independent sources of information to determine the location of the UAV and nearby objects, for example by combining GPS, LIDAR, visible spectrum video, and microwave ranging the drawbacks and failure modes of each of these technologies can be mitigated. A reflective surface may cause erroneous readings for the LIDAR and video systems, but not the microwave ranging.

### **2.3.3 Asymmetric Loading**

Significant attention must be given to the ability of the smaller UAV to handle asymmetrical loading, as the operation of the manipulator arm and management of off-centre payloads will be the primary mode of operation.

### **2.3.4 Management of Umbilical Cable**

The relative position of the lifting-gas support vehicle UAV and the smaller UAV generally determines the path of the umbilical cable, however consideration must be given to the curvature of the cable due to cable slack in various scenarios to ensure that the cable does not strike or tangle with nearby objects, structures, or the rotors of the smaller UAV.

### **2.3.5 Failure Modes**

A thorough treatment of failure modes of the entire system must be given in order to anticipate and prepare against catastrophic failures. Some of the scenarios which must be considered are listed below.

#### **2.3.5.1 Collisions**

The consequences of a collision with the structures being operated on, or other objects, people, or vehicles must be considered. In these scenarios, limiting the risk to the objects collided with should be the primary concern, and ensuring safe recovery after the collision a secondary concern.

#### **2.3.5.2 Rotor Failures**

The rotor system consists of the propeller, motor, and Electronic Speed Controller (ESC). Propeller failures can include partially damaged or deformed which reduce

efficiency and induce vibration, or completely failed propellers in which case no more lift is generated by the rotor. Motor failures can include bearing failure, motor shaft bending, magnet delamination or demagnetization, and failure of the motor winding insulation due to excessive current and overheating. ESC failures can include overheating and failure of semiconducting components. Most of these rotor failures result in catastrophic failure of the entire system, and can be mitigated by taking steps to reduce the likelihood of the failure of the individual systems or by using multiple redundant rotors as in the commonly used X8 octo-copter

#### **2.3.5.3 Flight Control System**

The flight control system uses sensor readings to maintain the desired position and orientation of the UAV. Failure of the flight control electronics or firmware is catastrophic. A significant subsystem of the flight control system is the IMU, which supplies crucial information about orientation and angular rotation rates. Similarly to rotor failures, these systems can be individually strengthened to reduce the likelihood of failure, but should also have redundant fall-back systems in the case that a failure does occur.

# Chapter 3

## Control Implementation

### 3.1 Overview

The control implementation consists of several subsystems. First, a description of the signal flow between the systems is presented, followed by a more detailed description of each subsystem. The control implementation for both the initial smaller prototype and for the OmniCopter used the same method except for the specifics of the control algorithms and the control of the horizontal rotors present on the OmniCopter.

An overview of the Control Implementation is shown in Figure 3.1. A modified motion capture system, called the BlackTrax Tracking System, was used to measure the position of several infrared (IR) LEDs on the UAVs. The software element of the BlackTrax system runs on a PC called the Tracking PC. The measured LED positions are fed back to another PC, called the Control PC, over wired Ethernet LAN. The Control PC calculates the control signals, which are then sent via USB to the Serial Pulse Position Modulation (PPM) Converter. The Serial PPM Converter converts the control signals from USB to PPM. The control signals are then fed into the RC Transmitter Module. The RC Transmitter Module transmits the control signals over

a 2.4 GHz wireless radio protocol. The RC Transmitter Module also accepts manual control inputs from a human overseer. The human overseer can allow the control signals from the Control PC to pass through the RC Transmitter Module by activating a foot switch, or take manual control of the UAV through the RC Transmitter Modules control joysticks. When the foot switch is released the UAV is under manual control. The UAV receives the wireless control signals from the RC Transmitter Module and controls the velocity of its rotors. The UAVs rotor speeds influence its position and orientation. The Control PC is informed whether manual control is activated by the RC Transmitter Module. This takes place over the same USB link as the control signals transfer over. It is shown using a separate arrow in the diagram for clarity.

## 3.2 BlackTrax Motion Capture System

This system was used for both prototypes to measure the position of two points on the body of the UAVs in order to determine their position and yaw-angle. Figure 3.2 depicts the position of the tracked points on the two prototypes. The tracking system consists of an Optitrack motion capture system, produced by NaturalPoint, augmented with BlackTrax hardware produced by CAST Group. The BlackTrax hardware augmentation improves the performance of the motion capture system. BlackTrax hardware consists of beacons and a timekeeper. Figures 3.3, 3.4, and 3.5 depict the motion capture system components. The interaction of the BlackTrax components of the tracking system is shown in Figure 3.6. One beacon can support three infrared Infrared (IR) LEDs. The BlackTrax timekeeper ensures that the beacons' LEDs pulse in sync with the frame rate of the Optitrack cameras by transmitting a synchronization signal to the beacons. Each camera's shutter opens in sync with the other cameras and during the time that the cameras' shutters are open, the IR

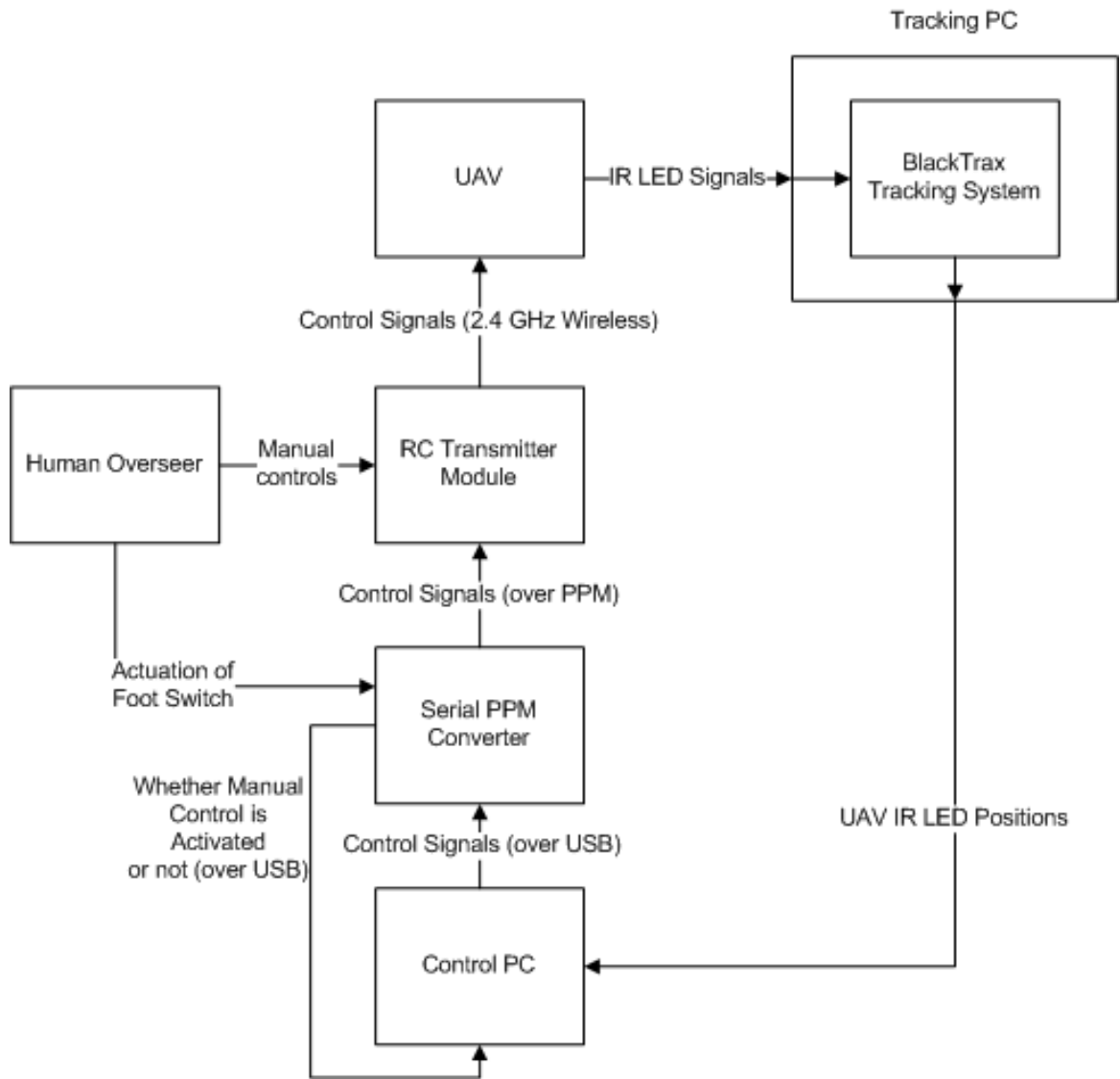


Figure 3.1: Overview of Control Implementation.

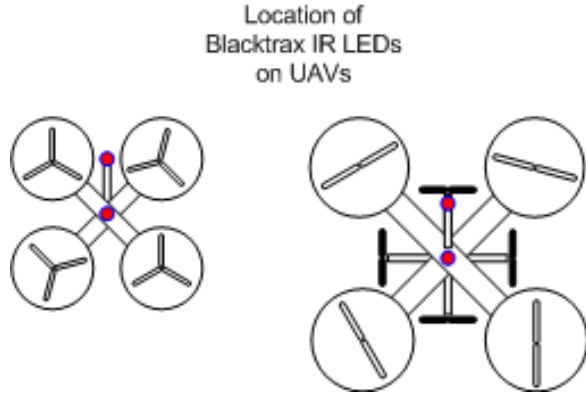


Figure 3.2: Location of position markers on UAVs.

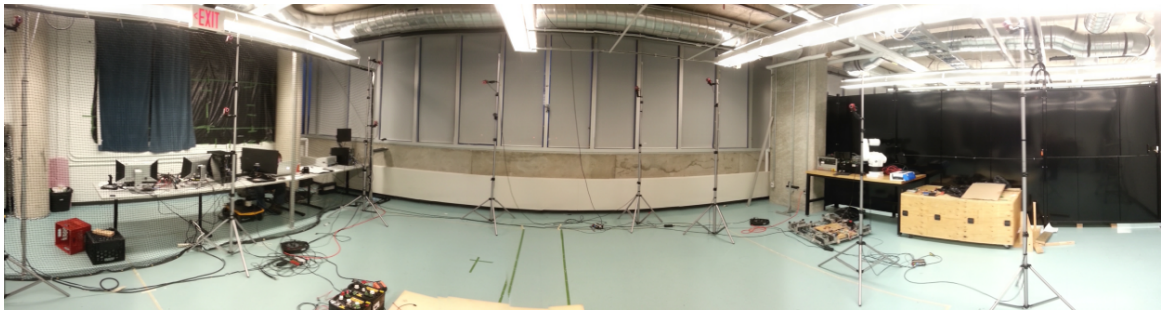


Figure 3.3: Motion capture testing area [5].

LEDs of the beacons either turn on or stay off. The IR LED's state during each frame represents one bit of a binary code. Across several consecutive frames of camera data, each LED is able to transmit a unique code which allows the LED to be distinguished from other LEDs.

The Optitrack software application which calculates the position of tracked points based on camera data is called Motive. Motive transmits the positions of the tracked points via a proprietary IP protocol called NatNet. An software development kit to facilitate use of the protocol is made available by NaturalPoint.



Figure 3.4: Two Optitrack USB cameras mounted on a telescopic tripod.



Figure 3.5: BlackTrax Timekeeper and beacons. One beacon is shown removed from its casing for weight reduction, with high-gauge wire soldered directly to the PCB.

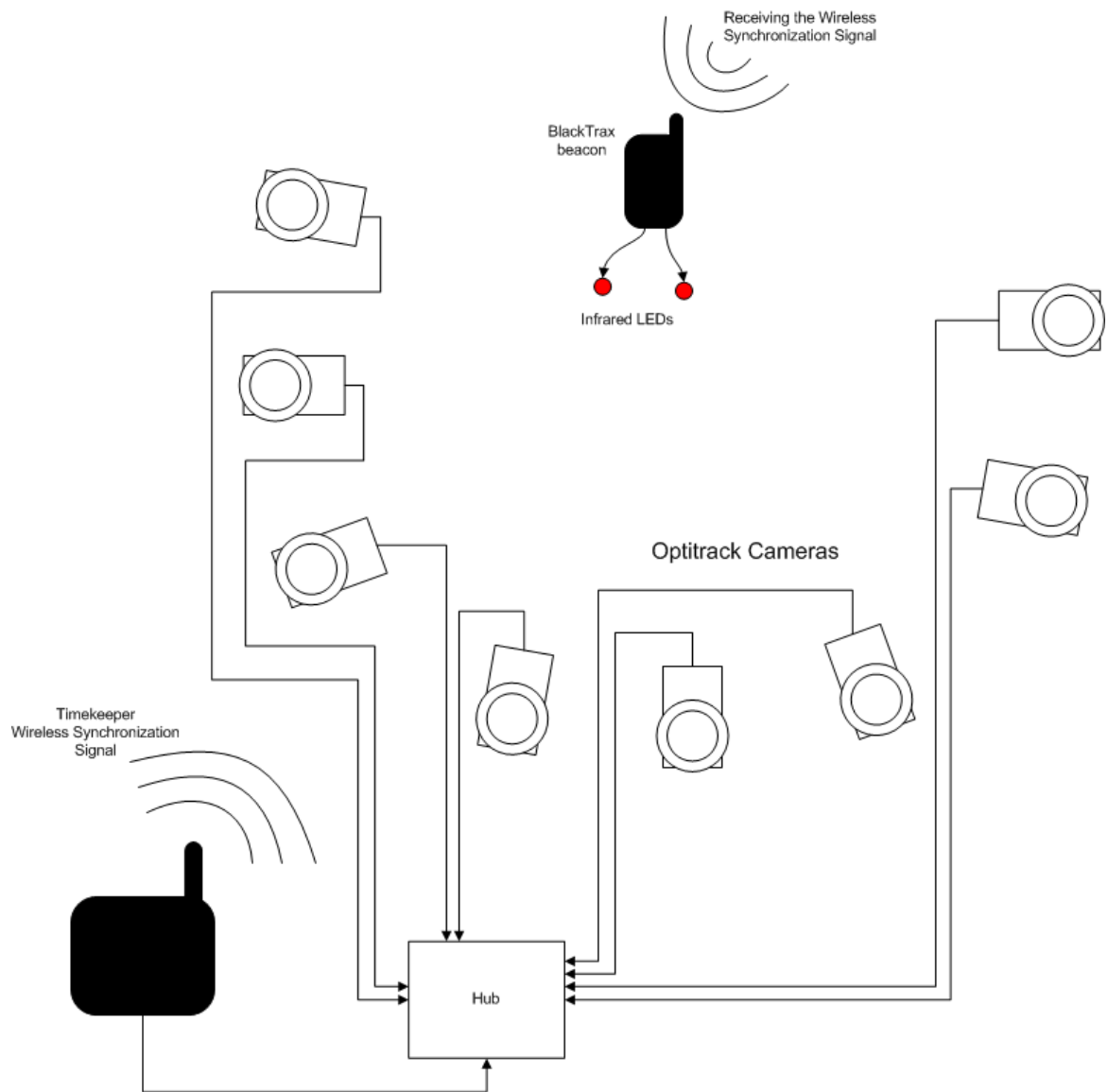


Figure 3.6: Representation of BlackTrax Motion Tracking System.

### 3.2.1 Advantages over Unmodified Motion Capture System

Traditionally, motion capture systems use reflective markers to track position. When at least two cameras detect a marker its position can be triangulated. In order to determine the orientation of an object, several small reflective infrared spheres are positioned in proximity to each. The objects can be distinguished from each other by recognizing the relative geometric position of the spheres. By ensuring unique geometric configurations for each set of spheres, separate objects can be distinguished from each other. The area in which tracking occurs is flooded with IR light allowing the reflective markers to be detected by the cameras. The cameras are sensitive to a narrow band of the IR spectrum. This approach requires careful control of IR lighting conditions in the area it is being used in to avoid saturating the cameras' sensors and getting erroneous signals from other reflective objects.

The first advantage of using the BlackTrax system is that since it uses IR LEDs instead of reflective markers, the area in which position tracking occurs does not need to be flooded with IR light to allow the markers to be detected. The markers can be detected directly since the LEDs are emitting infrared themselves. This allows the range of the system to be extended significantly before a signal is lost. This is useful in the case of experimentation in very large spaces. Furthermore, it is possible to use very bright and powerful IR emitters on the tracked objects and overpower the effect of the IR present in daylight. This means the BlackTrax system can be used outdoors and during the day.

The second advantage of the system is that the use of binary encoding across subsequent frames of camera data allows each marker to be distinguished uniquely from other markers. This means that if the LED is obscured and the position is temporarily lost, it can be easily identified and distinguished from other markers when it becomes

visible again. Only a single marker needs to be used to identify a point easily and uniquely.

### 3.3 Control PC

The Control PC contains a Robot Operating System (ROS) node which listens for NatNet messages on the Ethernet network. This ROS node is a modified version of the `mocap_optitrack` [41] node. The modification was made to allow handling the special NatNet message types used by the BlackTrax system. In the Motive software and the NatNet protocol these message types are called *active markers* and *active marker labeling*.

The modified ROS node transmits a `tf` [42] message which is received by the Control Node. A `tf` message is a type of message which provides coordinate frame information within ROS. The Control Node is further described in the Control System subsection. The Datalogging and display tasks shown in Figure 3.7 receive information from the Control Node, while the position and velocity goals for the UAVs are specified by the Position and Velocity Goals node. A block diagram of the Control PC components is presented in Figure 3.7.

### 3.4 Control System Algorithm

The control system for the OmniCopter generally consists of nested PID controllers. Control of orientation is independent of control of position, and uses two control loops, as depicted in Figure 3.8. It is implemented on an onboard Flight Controller. The same type of Flight Controller was used for both UAVs, and is available off-the-shelf. It is a MultiWii Pro and uses an Atmega 2560 Microcontroller Unit (MCU) as well as an onboard Inertial Measurement Unit (IMU), which consists of three orthogonal

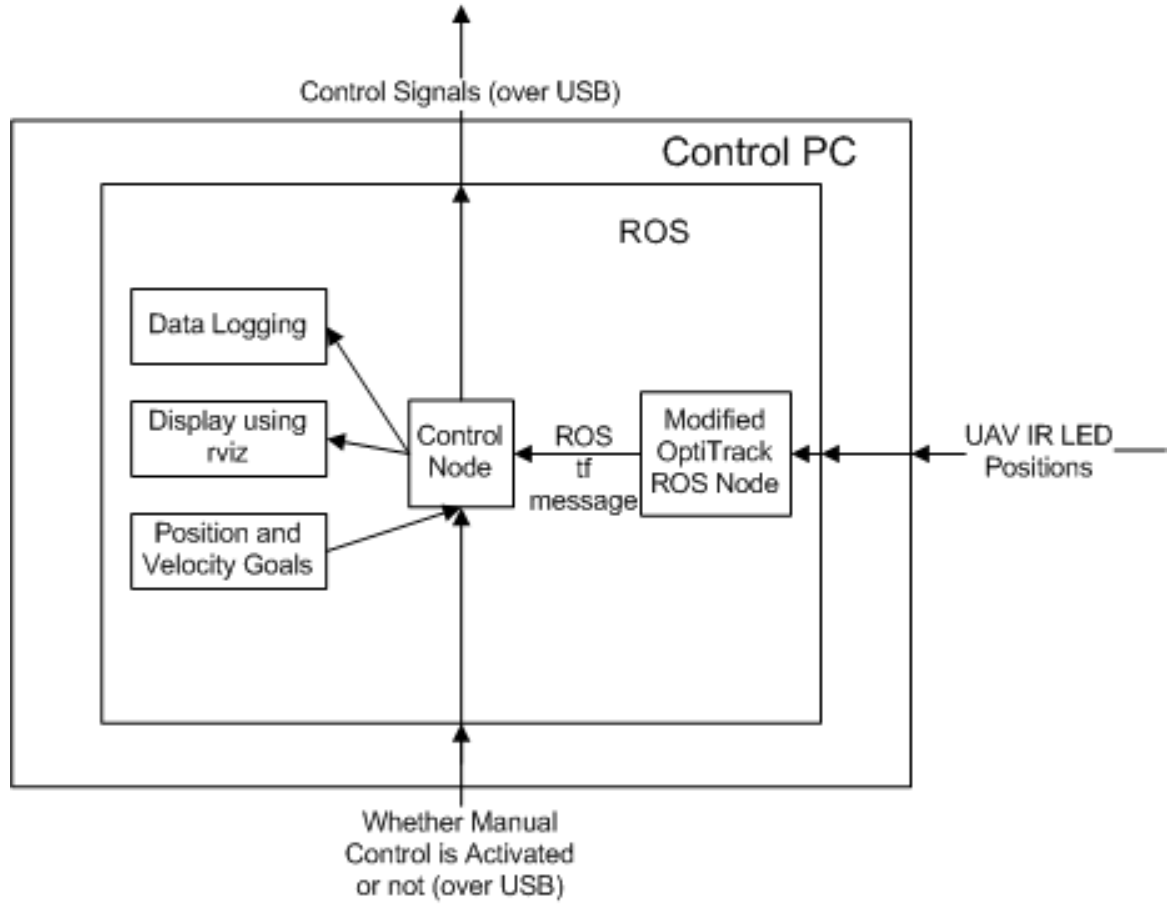


Figure 3.7: Diagram of Control PC functions.

accelerometers and three orthogonal rate gyroscopes. The inner control loop handles roll, pitch, and yaw angular velocity and the outer control loop handles roll, pitch, and yaw angular position. The MultiWii Pro Flight Controller was not modified aside from tuning the PID parameters to suit the size and characteristics of the UAV.

Figure 3.9 depicts the control of position for the X and Y position, and Figure 3.10 depicts the control of the Z position. The only difference between the two being that to control Z position only the average thrust of the 4 main lift rotors is used, with no compensation for any roll or tilt angle. For both the control of the X and Y position and the control of the Z position a nested control strategy is used in which the inner loop attempts to reach a velocity setpoint, and the outer loop determines that velocity setpoint. The velocity setpoint is proportional to the position error. Additionally, after a velocity setpoint is determined, it gets clamped to a reasonable maximum value so that a very large position error does not result in a very large velocity setpoint. These maximum velocities were chosen based on the size of the test area and speeds within the UAVs ability to accelerate to and decelerate from within the space. In practice, the clamping values used during experimentation and testing ranged from 10 cm/s to 40 cm/s for the Z direction and 20 cm/s to 100 cm/s for the X and Y directions.

In order to enable the OmniCopter to dock with a moving target, an additional input was added to the control algorithm. A target velocity can be specified, which is added to the velocity setpoint that gets generated by the error in position.

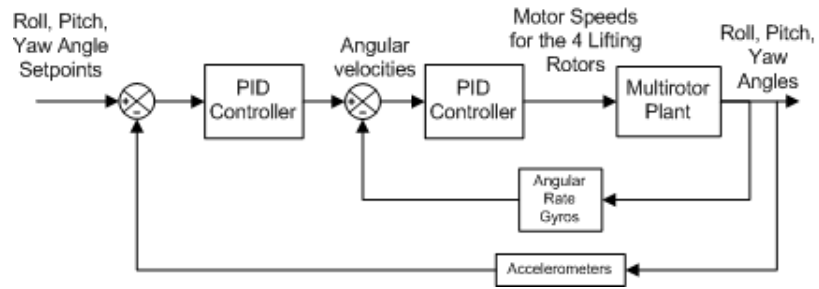


Figure 3.8: Control for roll, pitch, and yaw.

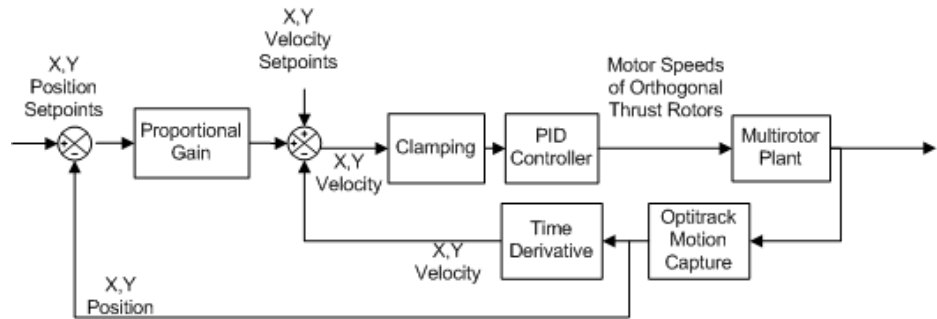


Figure 3.9: Control for X and Y position.

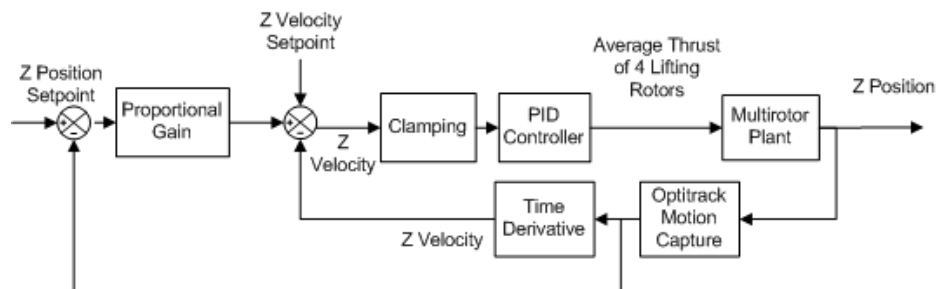


Figure 3.10: Control for Z position.

## 3.5 Serial PPM Converter and RC Transmitter Module

The Serial PPM Converter and RC Transmitter Module are closely tied and are described concurrently. The Serial PPM Converter takes USB signals and converts them to PPM. This was required because the RC transmitter uses PPM internally as a signal input to the radio transmission stage. By creating a conversion from USB to PPM it allowed the easy input of a signal from a PC to any radio controlled device, using the existing and proven RC technology. The conversion is handled by an Arduino Uno. The Arduino reads a set of 4 or 6 comma delineated RS-232 serial values received via the USB port. The initial prototype used 4 values corresponding to desired roll, pitch, yaw, and average thrust while the OmniCopter uses two additional values corresponding to thrust in the X direction and thrust in the Y direction<sup>1</sup>. These values are converted to PPM using existing software libraries and output on a data pin. The voltage of the signal is stepped down from 5 V to 2.6 V using a voltage-divider. The voltage step-down was done to match the voltage level of the signal which is normally inputted to the transmitter stage on the RC transmitter module. The Arduino Uno also senses the state of a manually foot activated switch. When the switch is depressed, the PPM control signals from the PC are connected to the input of the RC Transmitter Modules radio transmission stage using a relay. This relay also energizes a circuit which turns on an LED to indicate that autonomous flight is engaged. When autonomous flight is engaged a serial message is sent back to the Control PC to inform the controller. This is done to avoid integral windup of the integral terms of the PID control during manual flight. An image of the RC Transmitter Module is shown in Figure 3.11 and a schematic of the Serial PPM Converter is shown in Figure 3.12.

---

<sup>1</sup>These thrusts are in the X and Y direction in the body-frame of the OmniCopter.



Figure 3.11: RC Transmitter with modification to allow external PPM signal input.

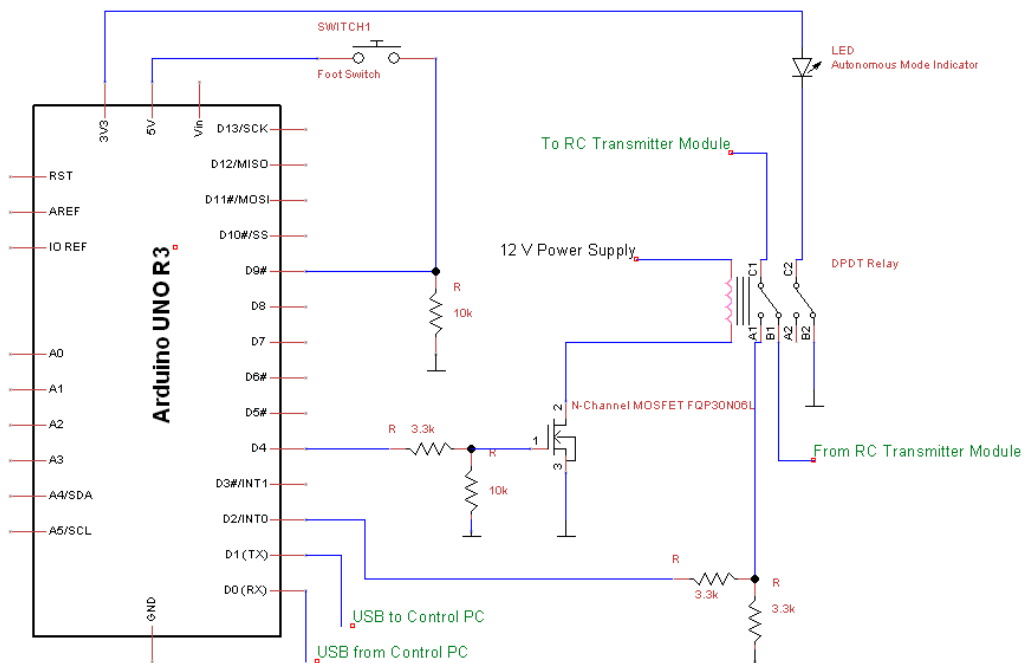


Figure 3.12: Electrical schematic of Serial PPM Converter.

When the foot switch is not activated the relay is not energized and the original signals generated by the manual controls on the RC Transmitter Module are passed through to the radio transmission stage.

## 3.6 UAVs

Both UAVs operate in fundamentally the same manner with the exception being that the OmniCopter has four additional rotors. The additional rotors on the OmniCopter take their inputs from the RC Receiver. The RC Receiver is the device on the UAVs which receives the 2.4 GHz RC signal from the RC Transmitter. The signal is decoded and converted into 6 separate Pulse Width Modulation (PWM) signals. These PWM signals are transmitted via servo cable. This is a digital signal in which the significant portion is the period of time during which the signal pulse is high. The upper and lower limits of the on-time of the pulse varies somewhat depending on the manufacturer of the components being used. The value can go as low as  $800 \mu\text{s}$  and as high as  $2,100 \mu\text{s}$ , but usually remains within  $1,000 \mu\text{s}$  to  $2,000 \mu\text{s}$ . The PWM signal is passed from the RC Receiver to the ESCs. Generally, a shorter PWM pulse indicates less power while a longer one indicates more. The ESCs which power and control the orthogonal thrusters on the OmniCopter were programmed with firmware capable of bi-directional operation. This means that a pulse-width of  $1500 \mu\text{s}$  corresponds to no power to the motor, rather than mid-range power. A value less than  $1500 \mu\text{s}$  indicates reverse thrust, while a higher power indicates forwards thrust.

The ESCs on the right-side of Figure 3.13 do not use bi-directional ESC firmware. The right side of the figure depicts standard quadrotor methodology. The control signals are received by the RC Receiver and decoded into PWM signals. There are four channels of information. These channels represent a desired roll angle, pitch

## UAVs

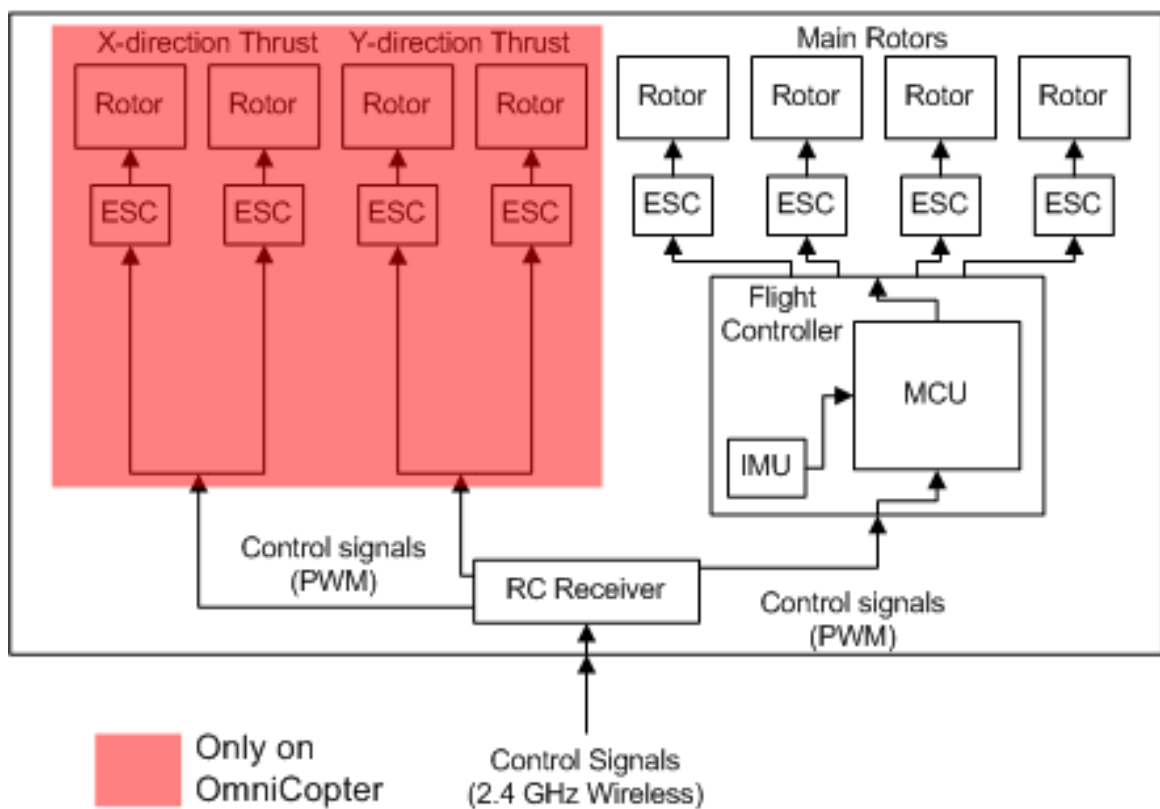


Figure 3.13: Block diagram describing the UAVs.

angle, yaw rate, and average thrust generated by the four main rotors. The Flight Controller reads these signals and controls the four main rotors to achieve the desired roll, pitch, yaw, and average thrust. The Flight Controller measures values using its IMU and uses the measured values to calculate the UAV's orientation relative to gravity and the nested PID controller for orientation is used to achieve the desired roll and pitch angles. A single PID controls yaw rate and open-loop control is used to generate the desired average thrust.

# Chapter 4

## Testing, Results, and Discussion

Testing for the OmniCopter consisted of several tests on the characteristics of the rotors, some initial flight testing to tune the controller PID parameters and qualitatively assess the prototype's flight capabilities, and station keeping tests first in calm conditions, then in the presence of simulated gusting winds. In the station keeping tests, the OmniCopter's performance was compared to the traditional method of control using roll and pitch. Demonstrations of the OmniCopter's capability to slowly approach and land on an inclined surface in a controlled manner were performed, and test flights demonstrating the OmniCopter's ability to match the position and velocity of a moving target were also done.

### 4.1 Rotor Tests

This section presents testing which was done on the main lift rotors and the orthogonal thrust rotors. This was done to quantify the characteristics of the actuators so that effective control could be applied. Primarily, it was of interest to quantify how great of a rate of change of thrust versus time could be achieved, as it is this parameter which determines how quickly a disturbance force can be compensated for. Also of interest was whether the approximate model for thrust force was accurate and how

ESC input commands related to motor output speeds.

### 4.1.1 Rotor Testing Setup

To perform the tests on the rotors a **Series 1580 Thrust Stand and Dynamometer** from RCbenchmark.com was used. An image of the thrust stand being used to test one of the OmniCopter thrust rotors is presented in Figure 4.1. The thrust stand uses strain gauges to measure the deflection of its aluminum frame, allowing thrust and torque to be measured. Motor RPM, supply current, supply voltage, motor temperature, ESC temperature, vibration (using a Micro-Electro-Mechanical-Systems (MEMS) accelerometer), and commanded ESC PWM signal are also measured. An application is available from RCbenchmark.com to interface with the test stand hardware. The application can display plots of the measurements in real-time as well as record data.

### 4.1.2 Validating Thrust Model

In [10], an approximate model is developed for thrust  $T$  as

$$T \propto \omega^2 \quad (4.1)$$

where  $\omega$  is the rotor angular velocity. Plots of thrust versus rotor RPM are presented in Figure 4.2.

It can clearly be seen that although the main lift rotor fits the quadratic model for thrust very closely, the orthogonal thrust rotor does not. A possible cause for the discrepancy may be rotor blade deformation at higher RPM.

Plots of thrust versus ESC input signal are presented in Figure 4.3. It can be seen in the plots that aside from a small dead-zone at the beginning of the range, both

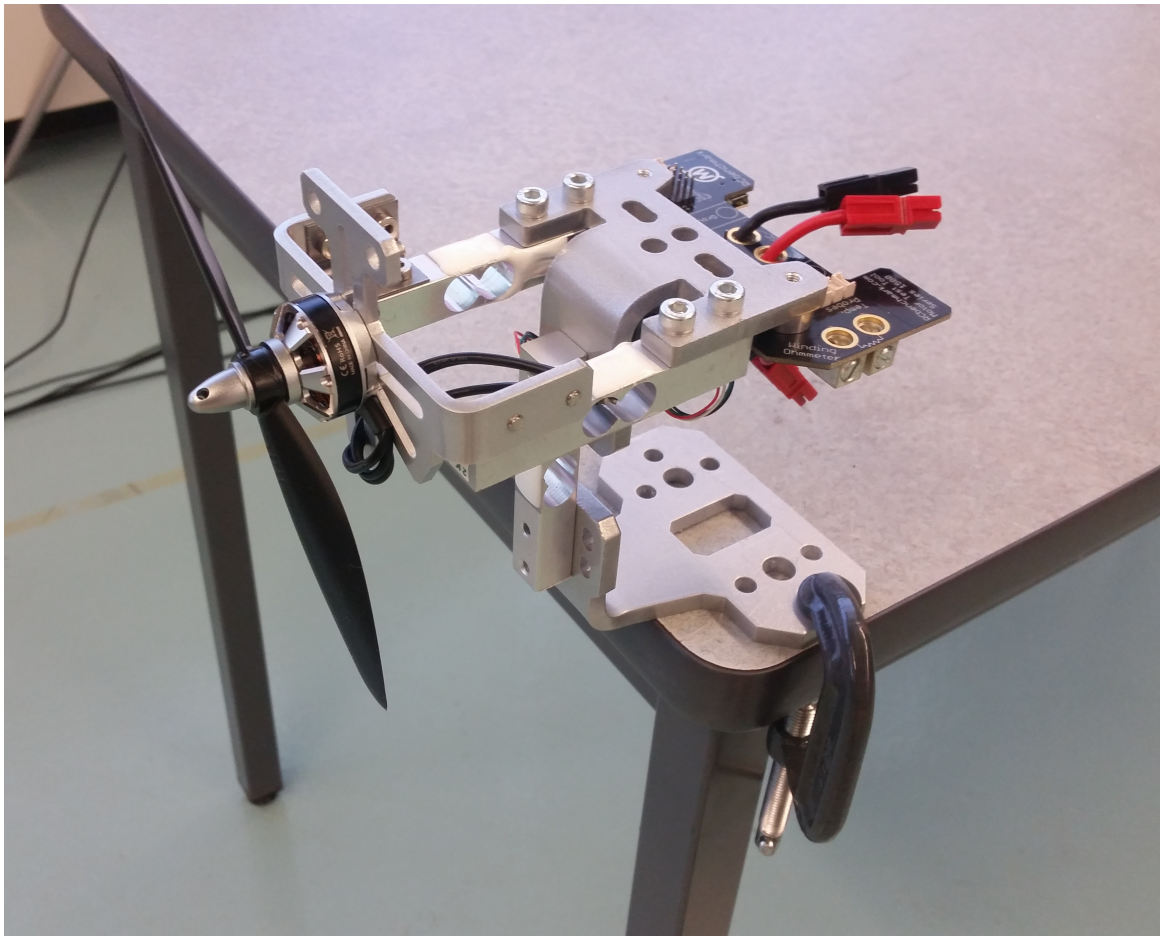


Figure 4.1: An orthogonal thrust rotor mounted on the thrust stand for testing.

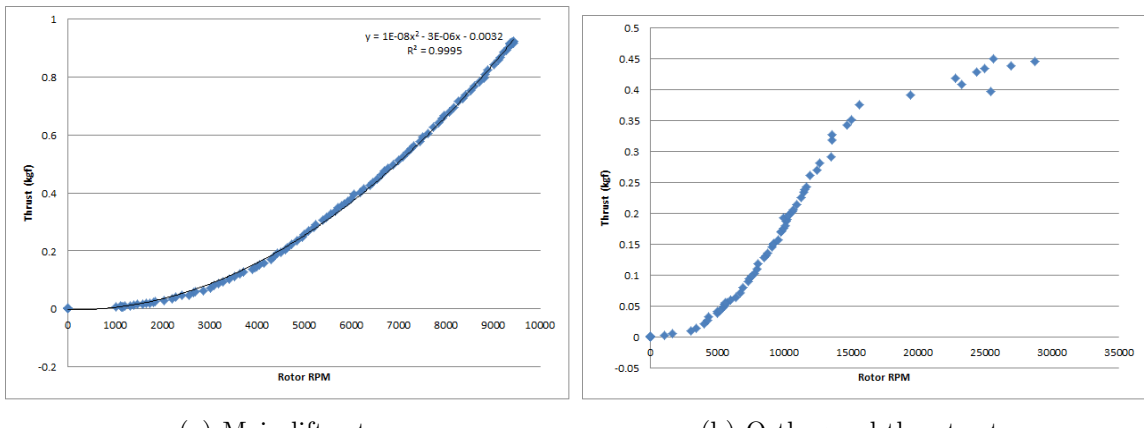
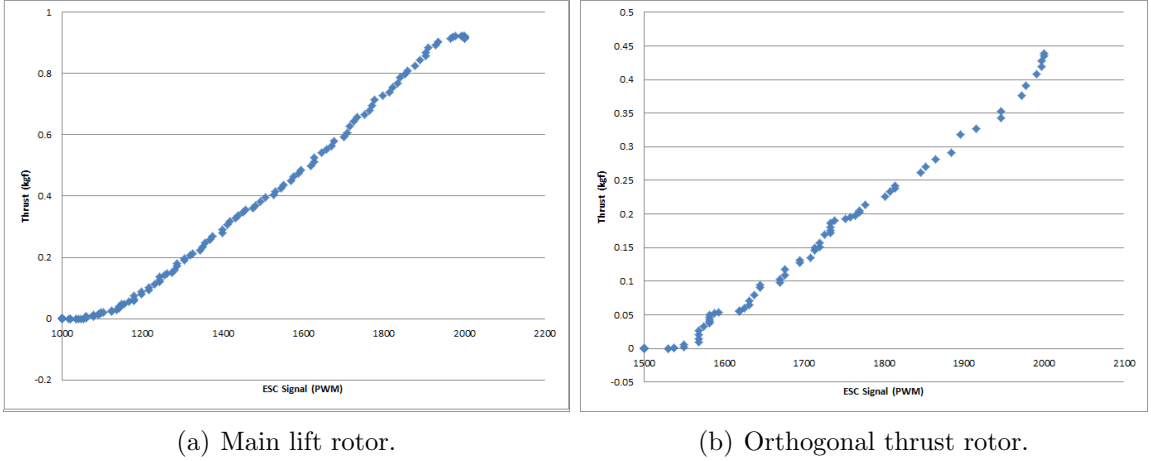


Figure 4.2: Thrust vs. RPM plots.



(a) Main lift rotor.

(b) Orthogonal thrust rotor.

Figure 4.3: Thrust vs. ESC input signal plots.

rotors have a fairly linear response to ESC input signal. This means that with a simple scaling constant, the control algorithm can treat rotor thrust and ESC signal equivalently without needing to perform an additional conversion before sending a command signal to the rotor ESCs. It should be noted that despite the discrepancy for the orthogonal rotor between the thrust model and actual behaviour, the input-output relationship from ESC to thrust is still linear.

#### 4.1.3 Thrust Rates

To measure the capability of the orthogonal thrusters to achieve a high rate of change of thrust, a square wave command input was given. This corresponded to alternating between large forward thrust and large reverse thrust. To achieve large changes in rotation speed, more motor torque is needed than would be for maintaining a constant rotation speed. The rotor's moment of inertia comes into play during changes in angular velocity. Figure 4.4 presents a plot of the orthogonal rotor thrust vs. time. For comparison purposes, a scaled and shifted plot of the command PWM input signal is overlaid over the values for thrust. It can be seen from the plot that it takes approximately 1 second for the rotor to switch from a large forward thrust to a large reverse thrust. It can also be seen that the magnitude of thrust is not symmetric for

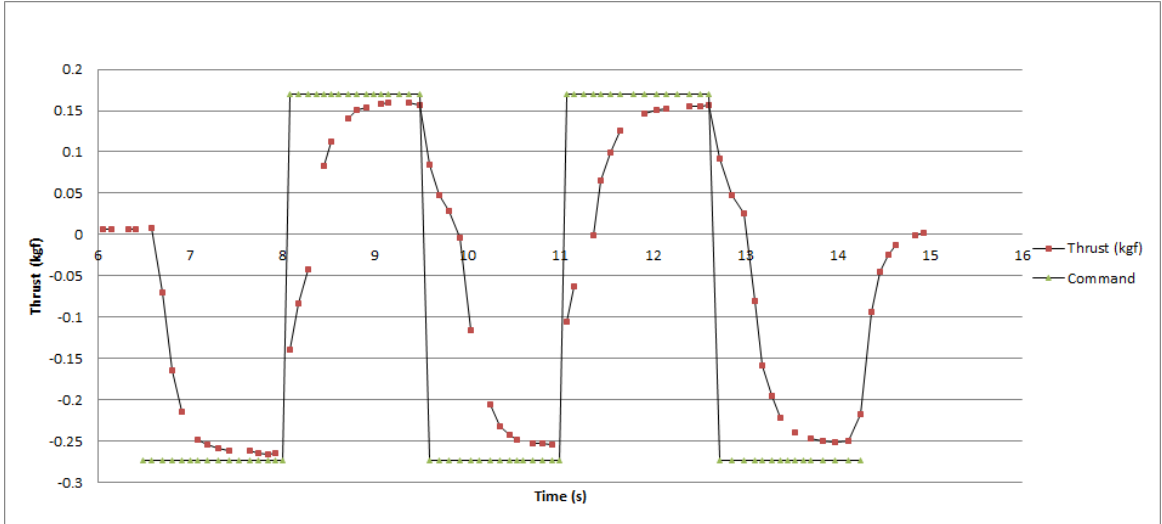


Figure 4.4: Test for orthogonal thruster maximum rates of change.

forward and reverse directions. This is because the propellers which were used are not designed for bidirectional rotation and are more efficient for one rotation direction. Because the orthogonal rotors are used in opposing pairs this asymmetry cancels out.

## 4.2 Initial Flight Testing

Initial flight tests were conducted during the tuning of the PID controller with promising results. No data was recorded during these tests but video footage demonstrating station keeping and controlled autonomous flight to waypoints was taken. This was accomplished using the orthogonal rotors to generate the necessary forces for translational motion and without the UAV needing to pitch or roll. Additionally, it was demonstrated that the OmniCopter can hover in place while maintaining a constant roll angle, something which would be impossible with a traditional multicopter or helicopter. Figure 4.5 presents an image of the OmniCopter hovering while in an inclined orientation. The largest angle that could be maintained at a hover was 20 degrees. Greater angles would require more powerful orthogonal thrust rotors with either larger diameter propellers or higher rotation speeds, however this may not be

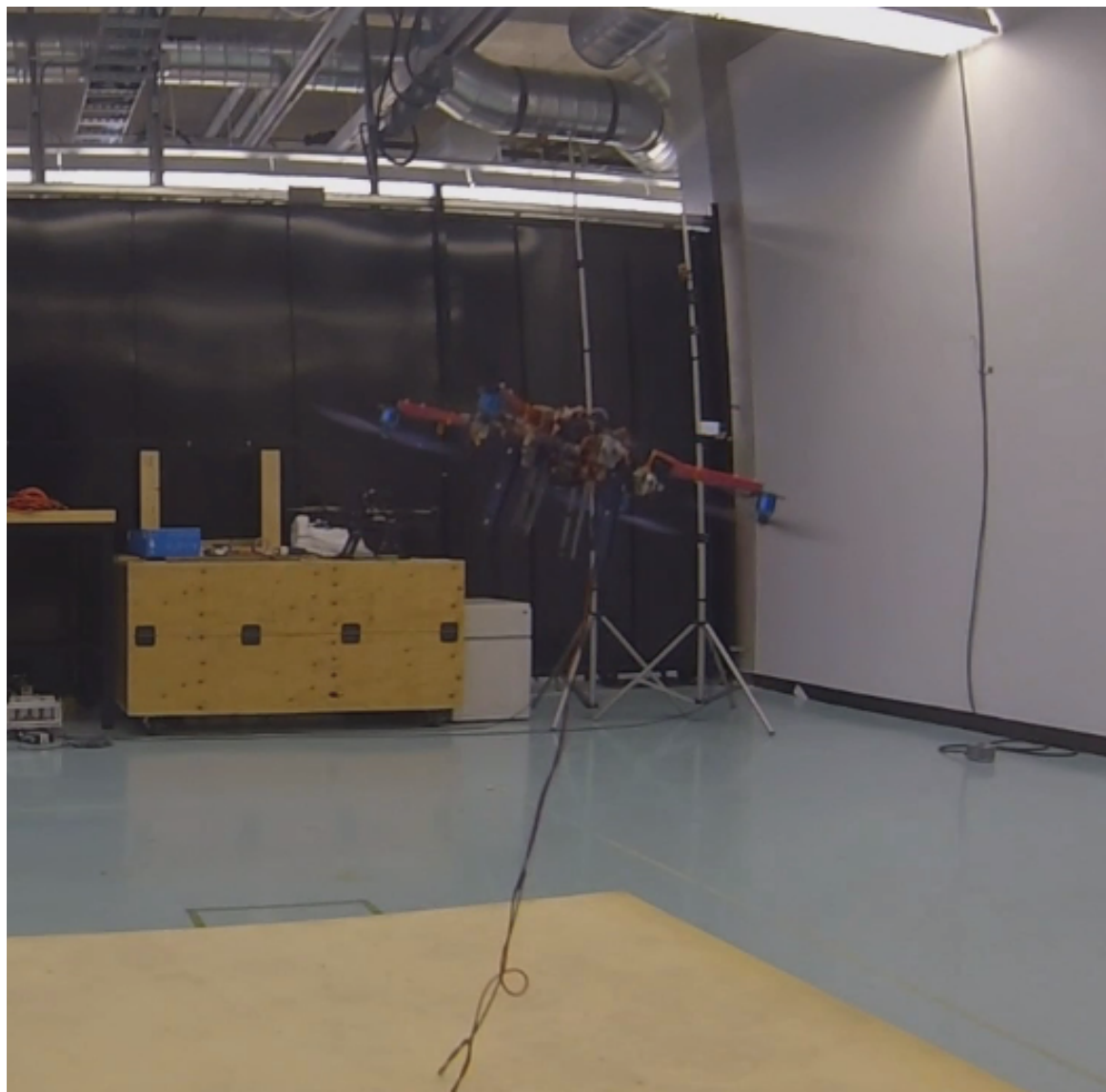


Figure 4.5: The OmniCopter hovering while maintaining a constant roll angle.

advantageous for the specific requirements of the OmniCopter, given that it is supplied power from above from an umbilical cord. Large roll and pitch angles create the risk of rotor strikes with the umbilical cable and so, in fact, translational flight while maintaining a level attitude is significantly advantageous.

## 4.3 Disturbance Rejection

To evaluate the OmniCopter's capacity for disturbance rejection it was compared against the traditional roll/pitch method of flight. The intention was to evaluate whether or not the OmniCopter has advantages over a traditional multirotor. To do this, an autonomous controller using roll and pitch (without using the orthogonal thrusters at all) to control position was applied to the OmniCopter and this was compared against the orthogonal thruster control method. When using the orthogonal thrusters for control, a constant horizontal flight attitude was commanded.

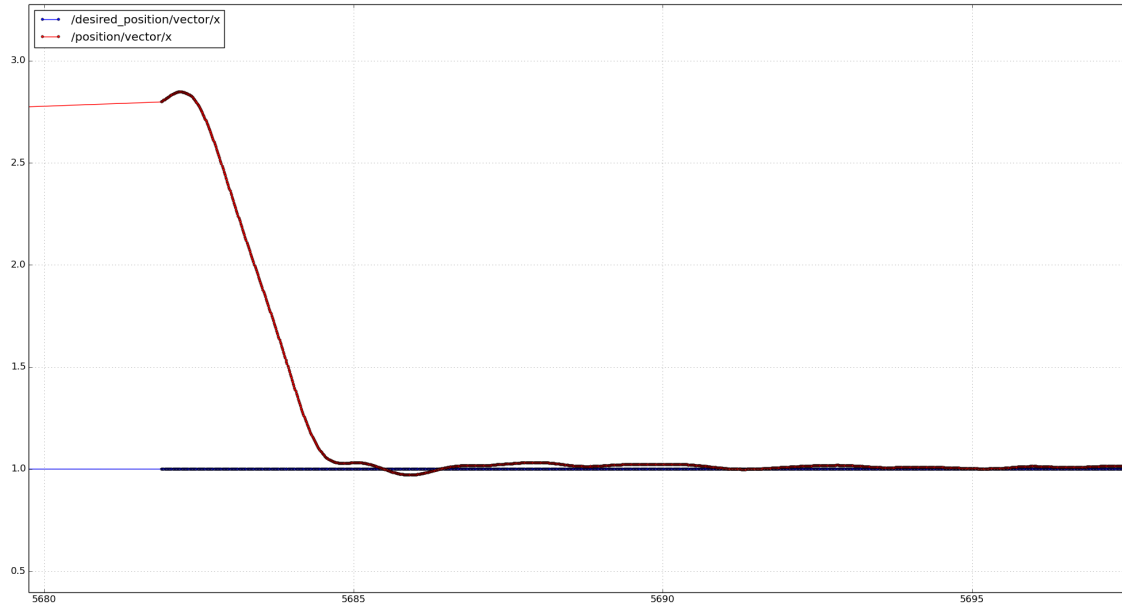
First, a set of tests were conducted in calm conditions to set a performance benchmark. In these tests the OmniCopter was commanded to maintain a static hovering position, and the deviations from the commanded position were recorded. The station keeping test in calm conditions was done for both flight control methods. A second set of tests were conducted in simulated gusting winds induced by a large fan.

### 4.3.1 Station Keeping Benchmark Tests

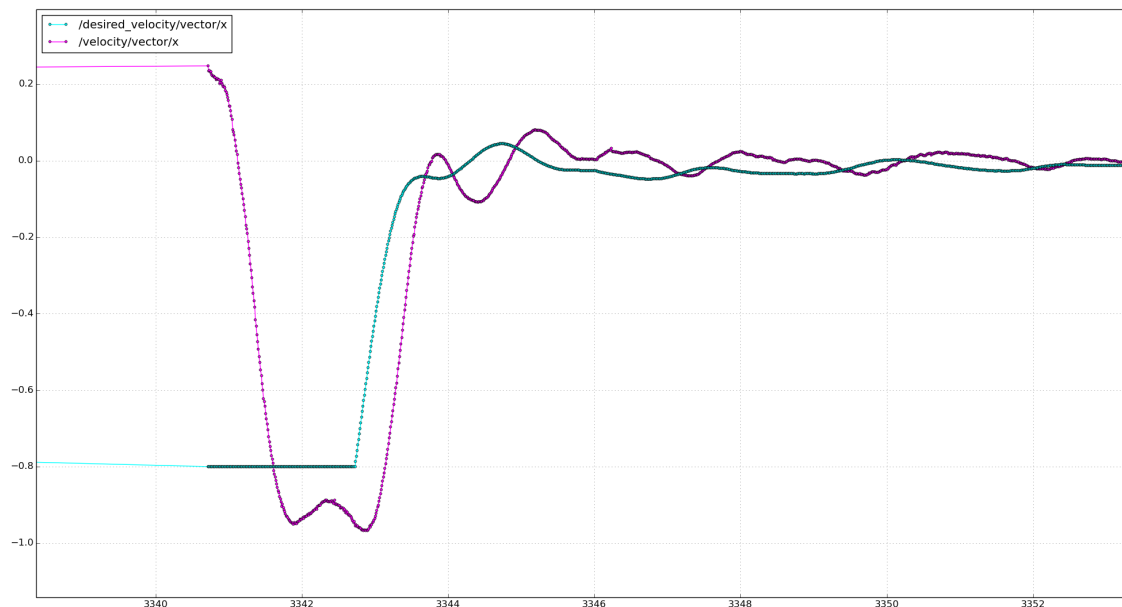
Figure 4.6 and Figure 4.7 show plots of the position and velocity in the X direction of the OmniCopter moving to and maintaining a static position under the roll/pitch control method and the orthogonal thruster control method respectively.

Figure 4.8 shows a side-by-side comparison of the two flight control methods. These are enlarged sections of the same tests once the OmniCopter reached the setpoint. It can be seen in the plots that both flight control methods are able to maintain position within approximately 2 cm of the target position.

It is not entirely surprising that both flight control methods would perform equiv-

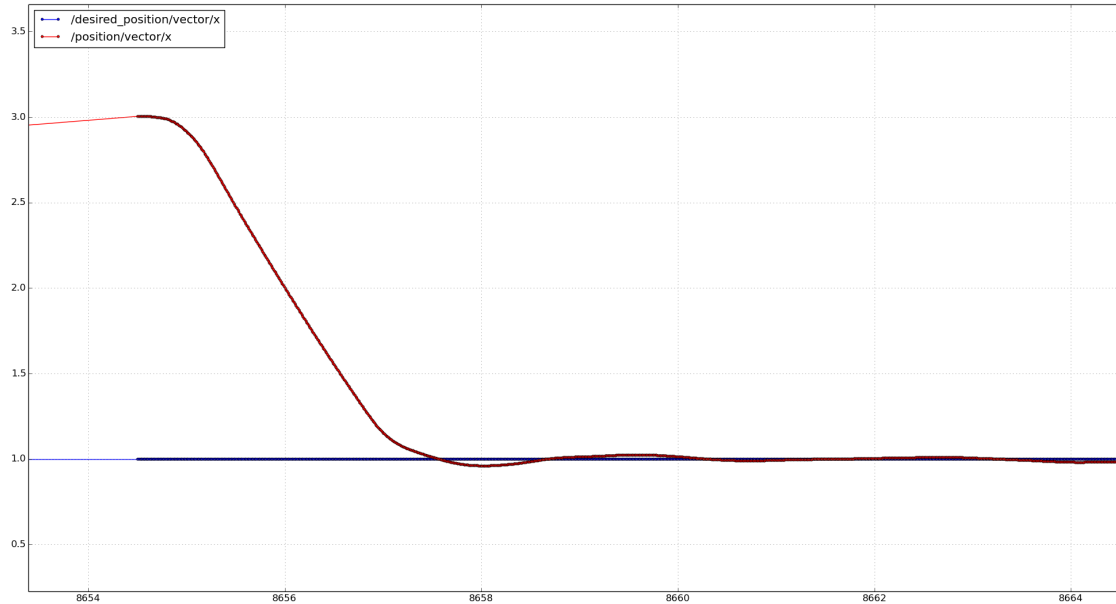


(a) Position vs. time.

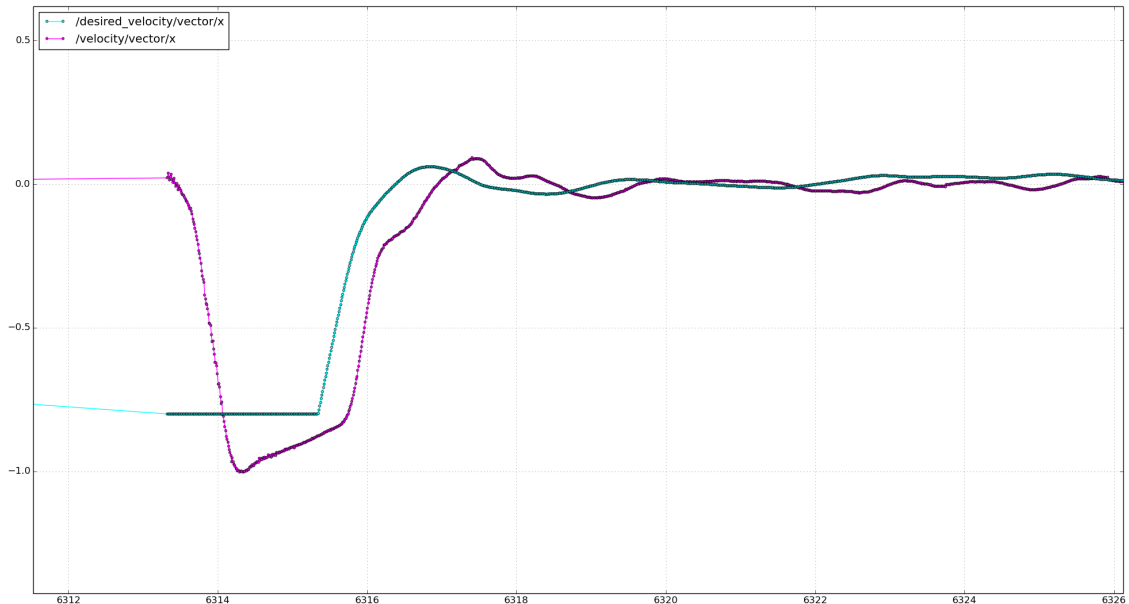


(b) Velocity vs. time.

Figure 4.6: Control using the traditional roll/pitch control method.

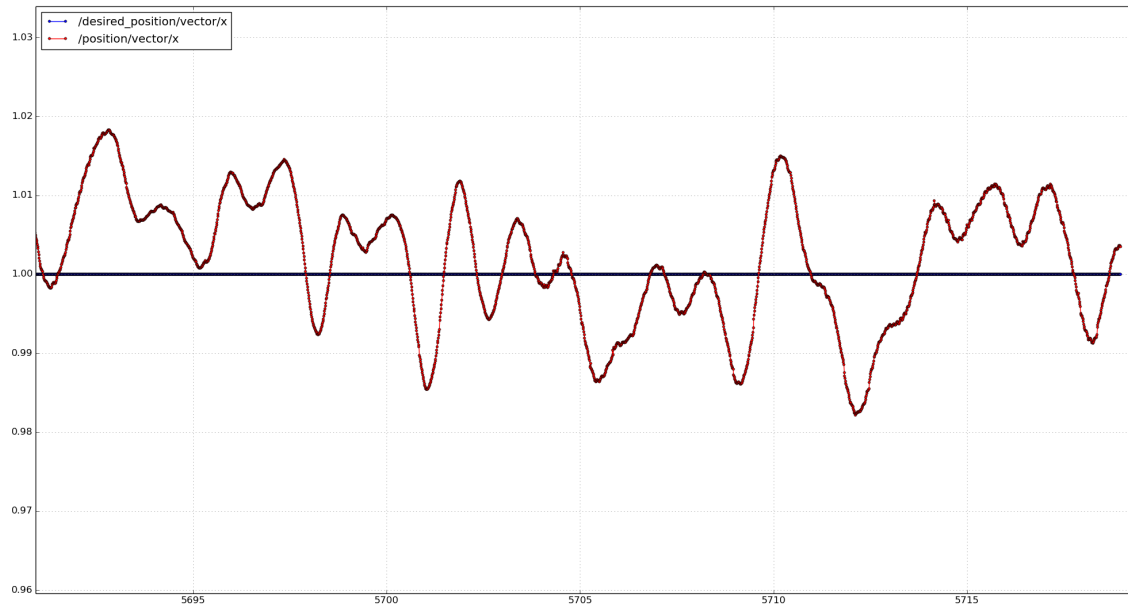


(a) Position vs. time.

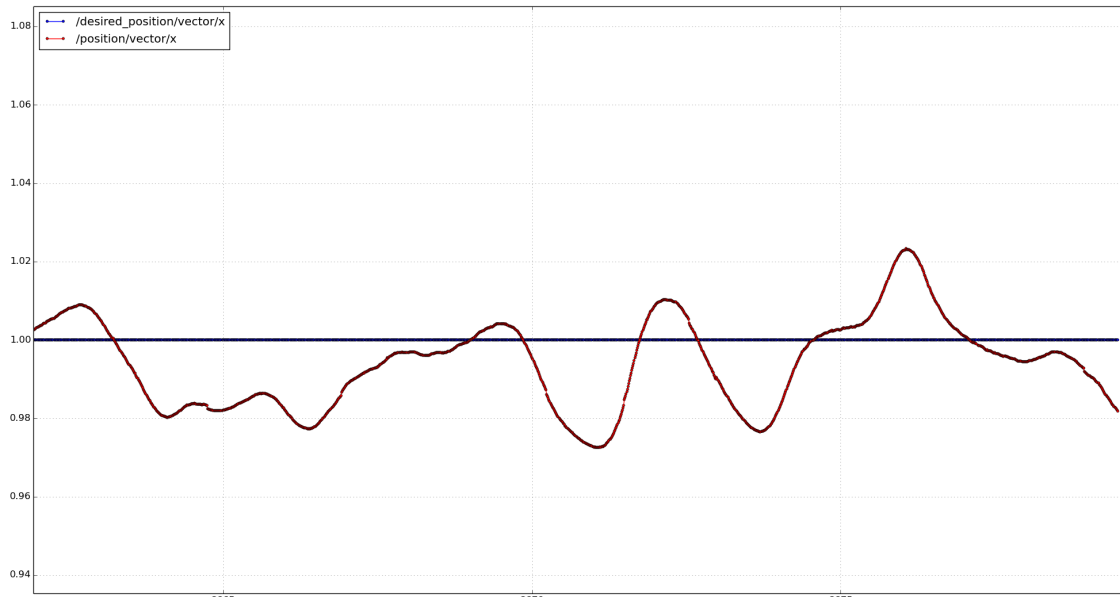


(b) Velocity vs. time.

Figure 4.7: Control using the orthogonal thruster control method.



(a) Position vs. time for traditional roll/pitch control method.



(b) Position vs. time for orthogonal thruster control method.

Figure 4.8: Enlarged sections of station keeping in calm conditions comparison test.

alently in the absence of disturbances. The orthogonal thruster control method is expected to have an advantage in being capable of responding to disturbances more promptly, however, in the absence of disturbances other sources of error affect both flight control methods equally. Some such potential sources of error are noise and inaccuracies in the position measurement system, latency in the data flow from sensing to actuation, and delay arising from the averaging filter used to estimate velocity from successive positions reported by the position measurement system.

### 4.3.2 Station Keeping in Gusting Winds

In order to simulate gusting winds for these tests, a large fan was constructed using a powerful RC outrunner motor. An image of the fan mounted on a table can be seen in Figure 4.9.

The fan was set to full power and an anenometer was used to measure air velocities at a point 2 m away from the fan. It was found that the fan generated a stream of air approximately 1 m wide with a fairly constant air velocity of 5 m/s at the centre. Fluctuations of approximately 0.5 m/s were observed at the centre of the air stream. As the anenometer was moved away from the centre, large fluctuations in air velocity were observed with velocities ranging from 2 m/s to 5 m/s. At a point 50 cm from the centre of the air stream the air velocity was relatively constant at 1 m/s. This velocity gradient is convenient for the intended station keeping test because if the UAV gets pushed away from the goal position in the centre of the air stream, it experiences a sudden change in force. Generating rapidly changing aerodynamic forces and evaluating the UAV performance was the goal for the test.

For this test, the UAV was commanded to fly to and maintain a position 2 m away from the fan in the centre of the air stream. Once the UAV was maintaining the

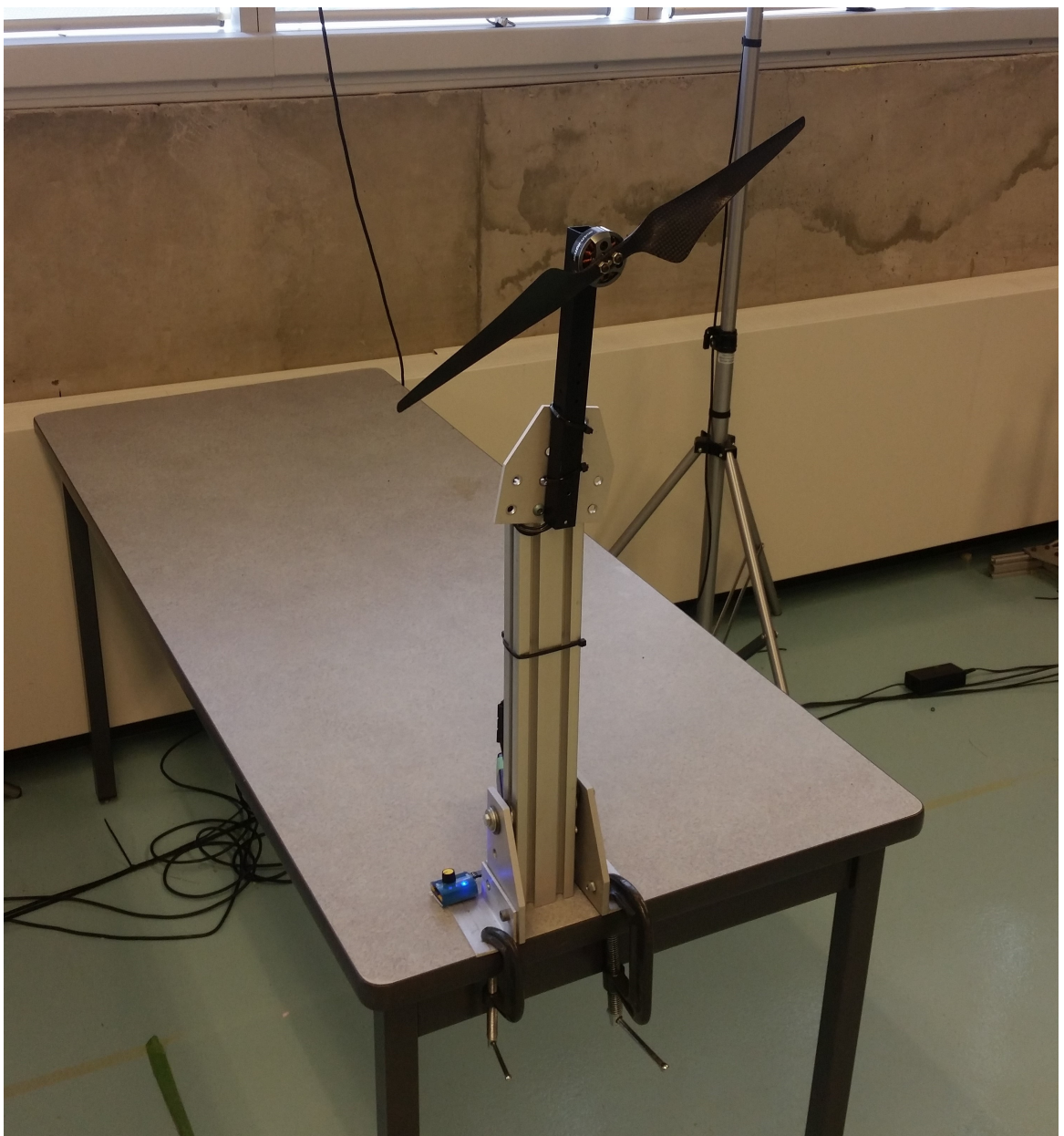


Figure 4.9: A large fan used to simulate gusting winds.

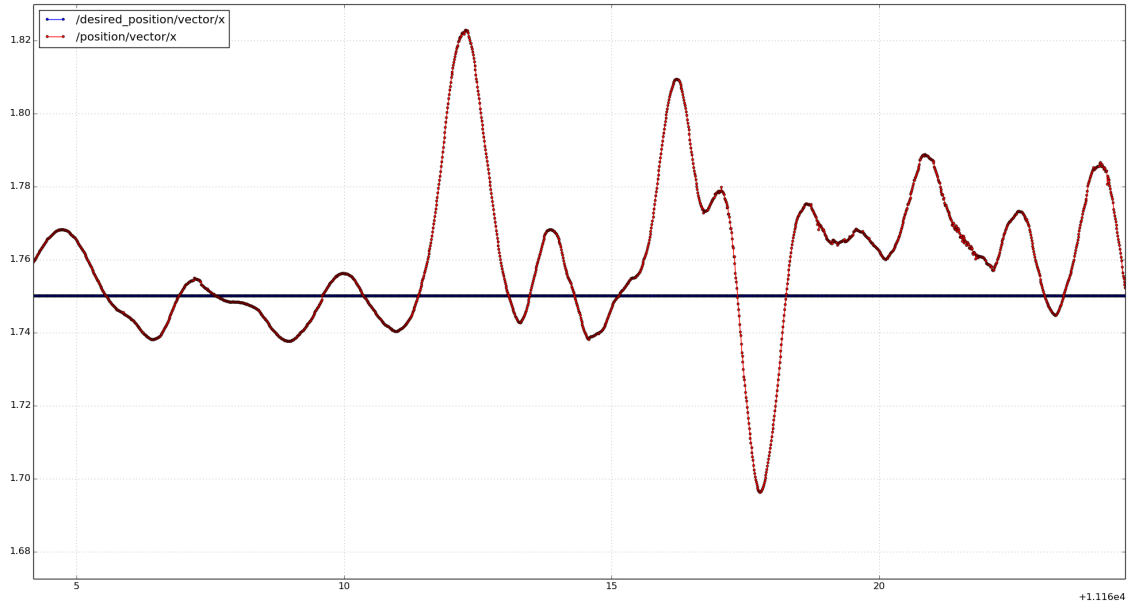
desired position the fan was manually engaged and the fan power alternated between full power and off. The fan was turned on and off once every two seconds to generate large time-varying aerodynamic forces.

Figure 4.10 presents plots of position for the station keeping in the simulated wind test. The range in position seen in the plot for the traditional roll/pitch method is from slightly below 1.70 cm to slightly above 1.82 cm. The range in position for the orthogonal thruster method is from 1.71 cm to 1.81 cm. The maximum deflection from the setpoint for the roll/pitch method is 7 cm and 6 cm for the orthogonal thruster method.

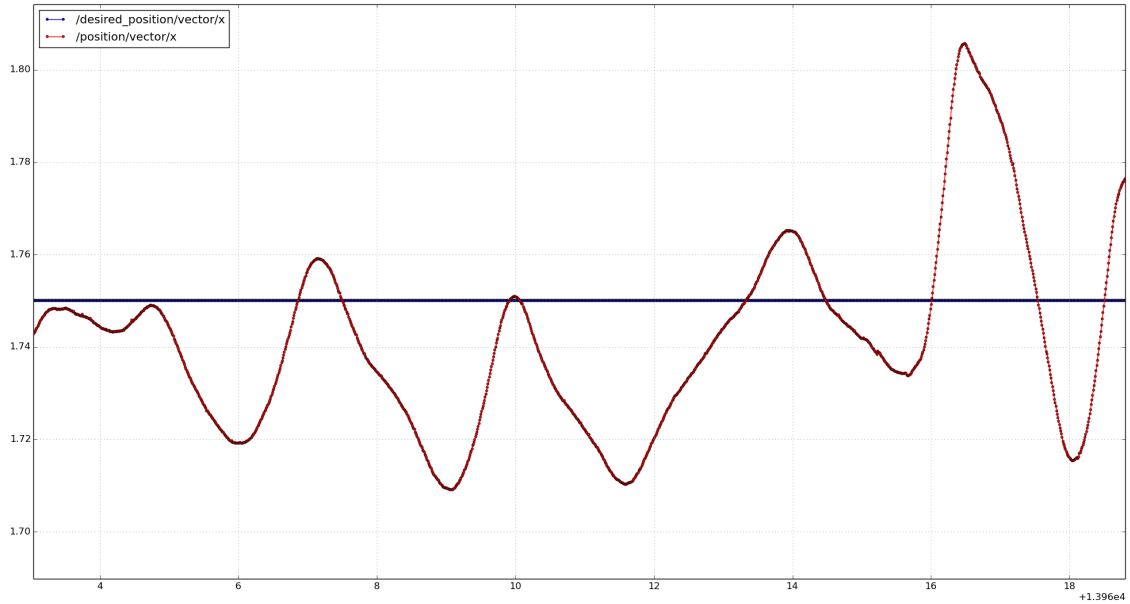
The reason why only a minor improvement can be seen in disturbance rejection with the OmniCopter may lay with the choice of variable speed rotors. The tests for thrust rates showed that it took one second to vary thrust from forward to reverse, which indicates that the actuators are not capable of generating a compensatory thrust quickly enough to react to disturbances well. Variable pitch rotors may offer improvements in performance here.

## 4.4 Landing on an Inclined Surface

Figure 4.11 presents an action-sequence image of the OmniCopter landing on an inclined surface. In this test the OmniCopter autonomously took off from rest, rose to a point 1.2 m above the takeoff position, then flew horizontally while maintaining a level orientation to a point above the inclined surface. Once above the inclined surface, it matched the orientation of the surface by pitching 20 degrees. While maintaining this pitch angle, it descended and landed on the inclined surface. Once it had landed, it then reversed the sequence of moves to return to the take-off point.



(a) Position vs. time for traditional roll/pitch control method.



(b) Position vs. time for orthogonal thruster control method.

Figure 4.10: Station keeping in simulated gusting wind.

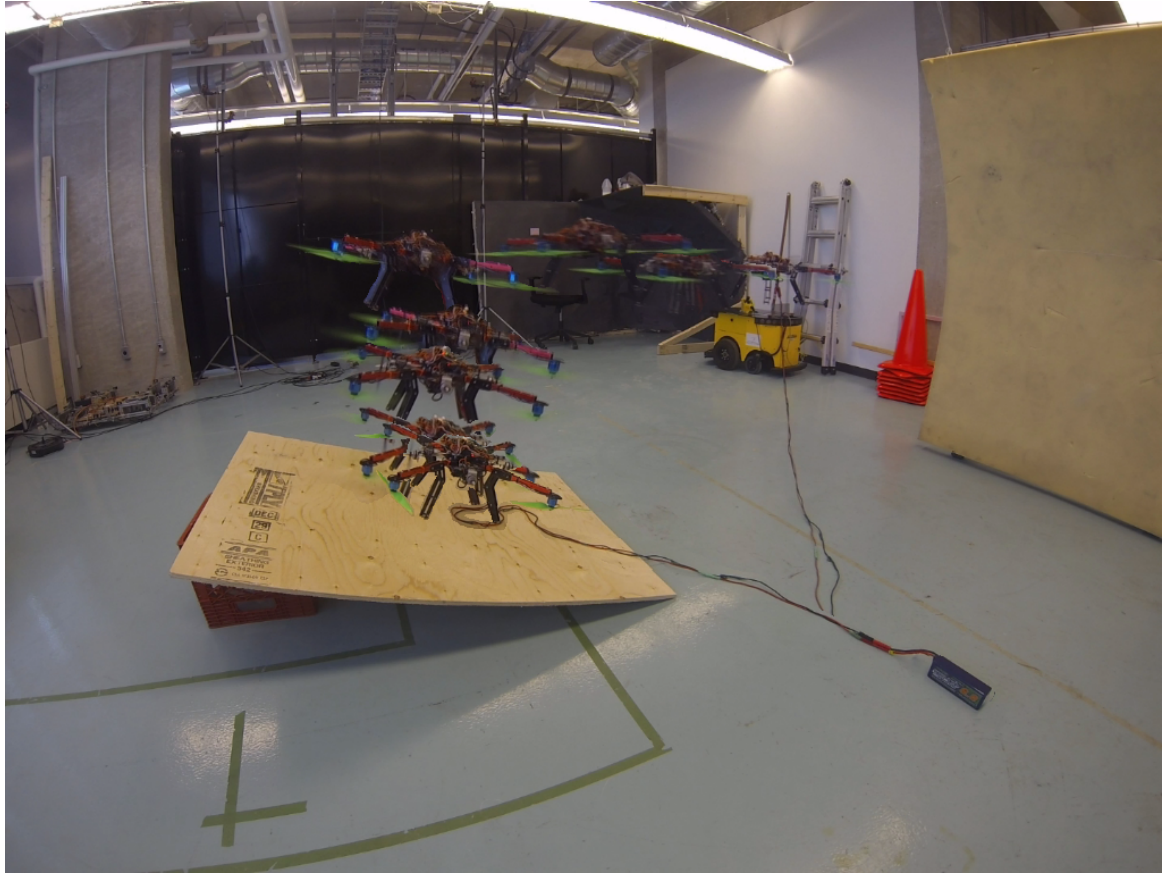


Figure 4.11: A action-sequence of the OmniCopter landing on an inclined surface (20 degrees incline).

This test demonstrates the increased flexibility of the OmniCopter as opposed to a traditional multirotor UAV. A traditional multirotor would risk the rotors striking the inclined surface during landing.

A second test was performed, this time with the inclined surface at an angle of 30 degrees to the floor. Figure 4.12 presents an action-sequence of the test. In this second test it was necessary to keep the orthogonal thrusters engaged once the OmniCopter had landed due to the greater angle of the incline. This allowed it to maintain stability on the surface and controlled the pitching moments induced by contact of the landing skids with the surface.

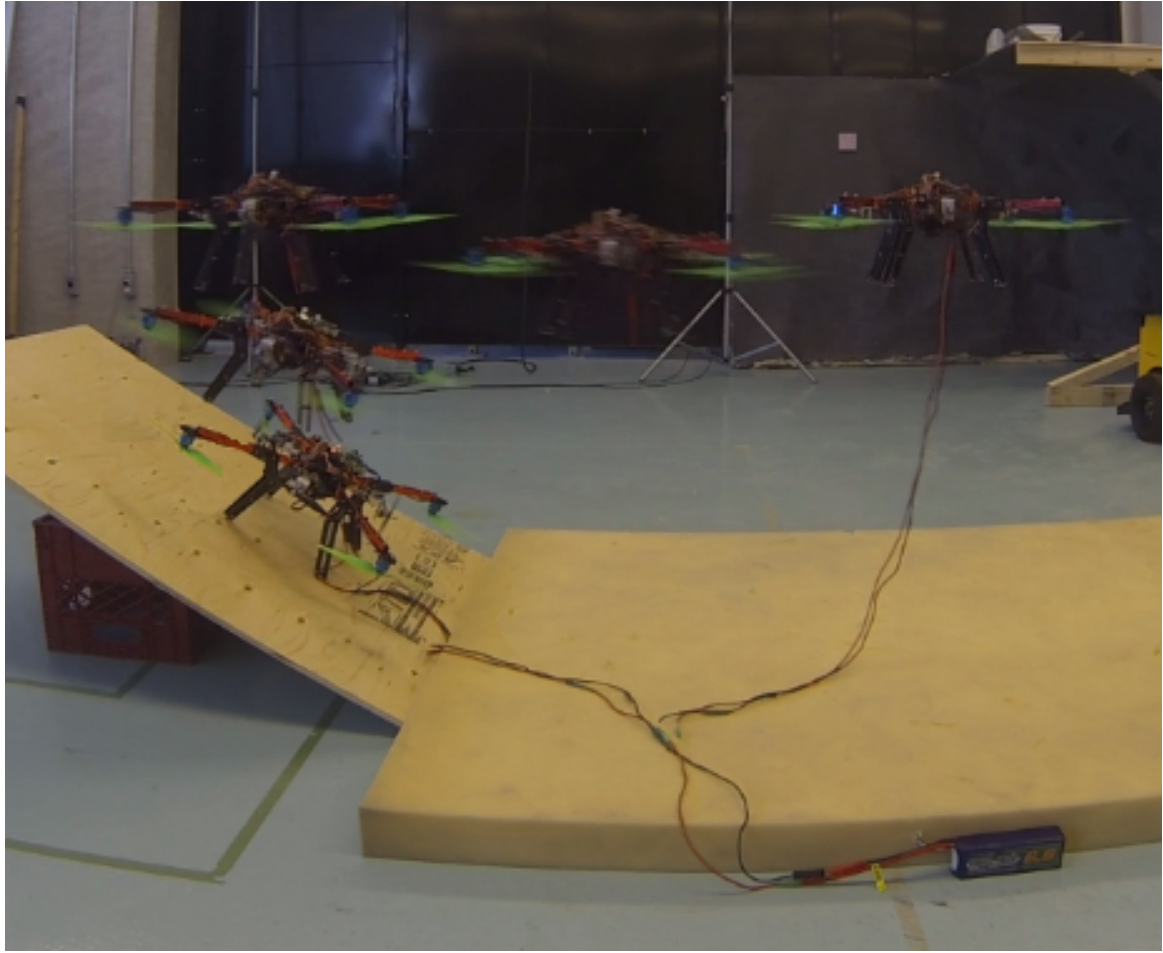


Figure 4.12: An action-sequence of the OmniCopter landing on an inclined surface (30 degrees incline).

## 4.5 Velocity Matching

In order to enable the OmniCopter to match speeds and dock with a moving target, an input for goal velocity was added to the control algorithm. This means that the velocity setpoint is composed of a term which is proportional to the distance between the OmniCopter and the goal as well as a term equal to the velocity of the goal. Without this additional term, the OmniCopter would always lag behind a moving target by a small amount.

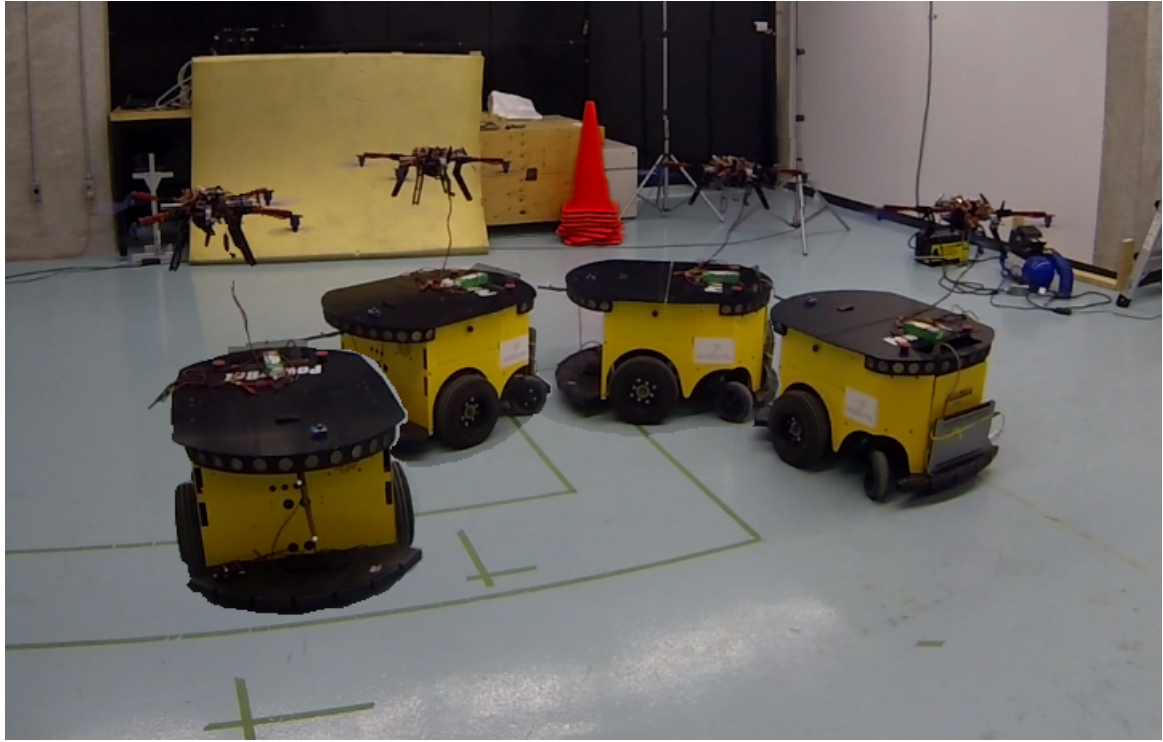


Figure 4.13: An action-sequence of the OmniCopter matching the position and velocity of a ground vehicle.

In order to test the algorithm, a robotic ground vehicle was commanded to drive in a circle within the tracking area. The OmniCopter was placed on top of the ground vehicle and would autonomously take-off from and match the velocity of the ground vehicle for the test.

Figure 4.13 depicts an action-sequence of the OmniCopter flying above the ground vehicle while matching its position and velocity, and Figure 4.14 presents an action-sequence of the same test, except that in this case the presence of the ground vehicle was simulated. A more rapidly moving goal position was given for the OmniCopter, which traveled at a rate of 50 cm/s.

Figure 4.15 presents plots of the position and velocity of the OmniCopter compared

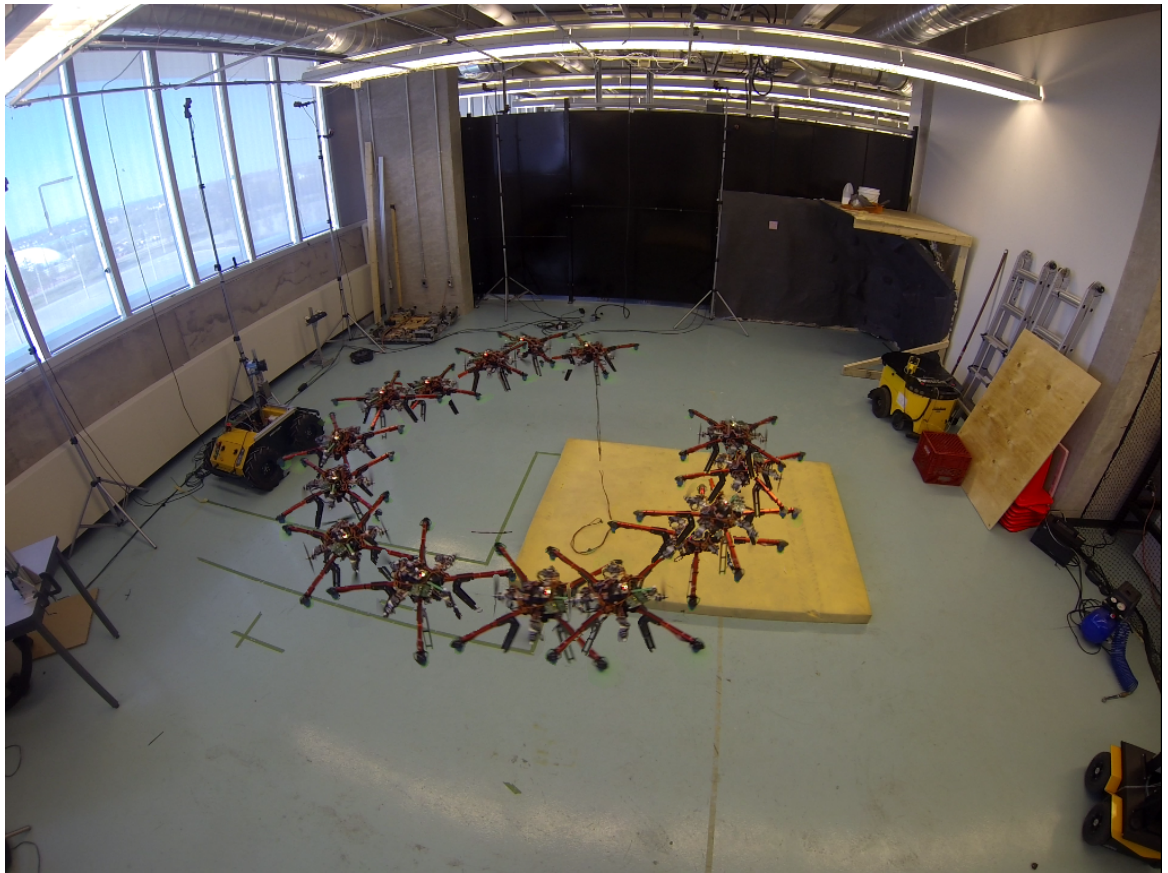
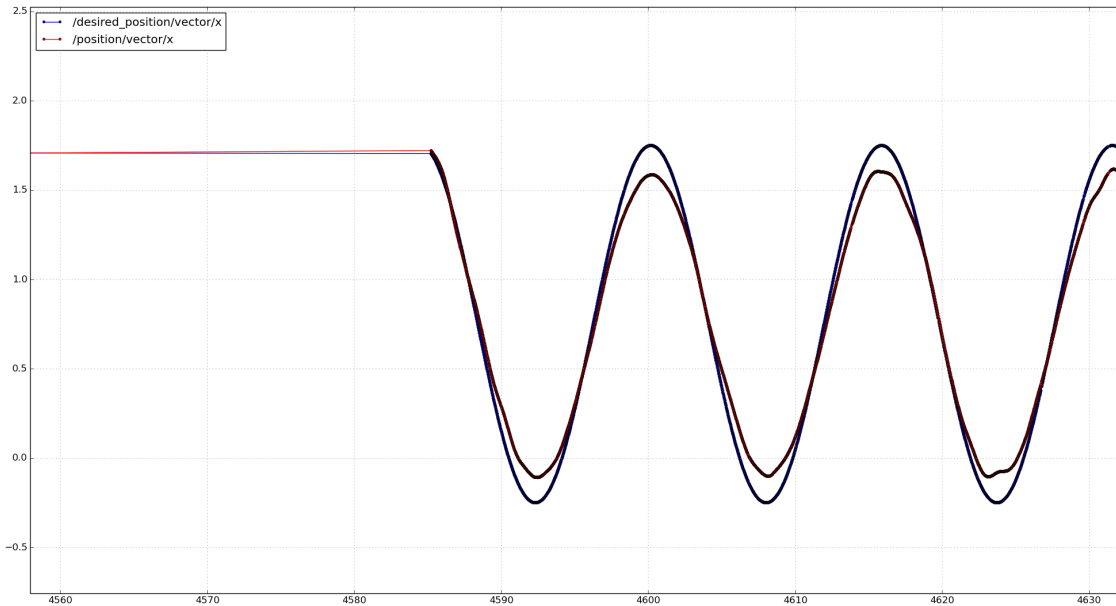


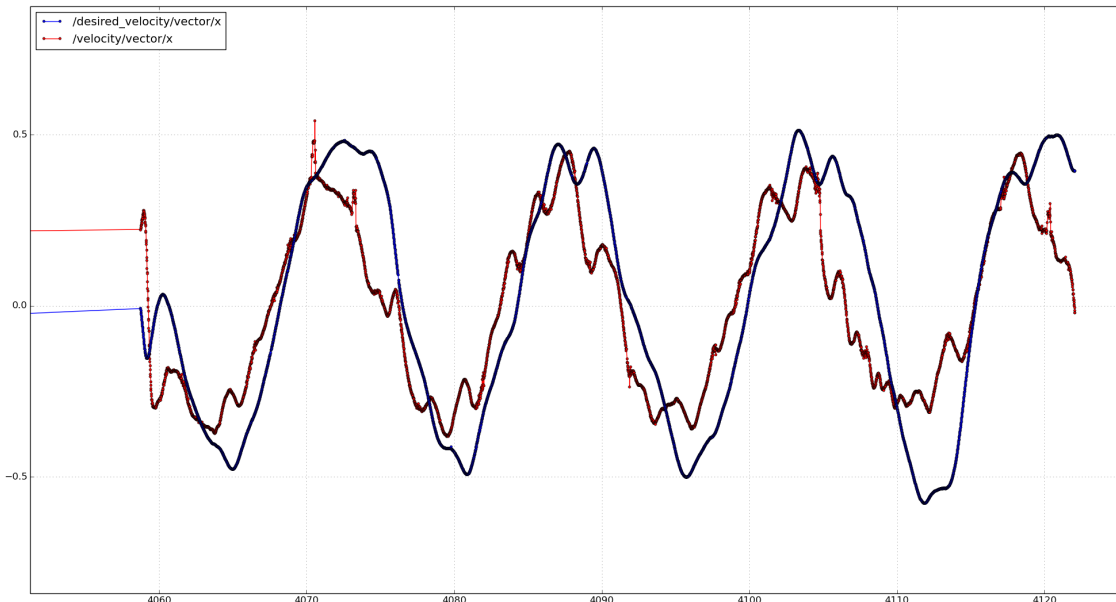
Figure 4.14: An action-sequence of the OmniCopter matching a moving goal position.

to the ground vehicle.

The results from this testing demonstrates that it is possible for the OmniCopter to closely match the position of a moving ground vehicle. This enables it to potentially dock with the ground vehicle even while the ground vehicle is in motion. The fact that the OmniCopter can do this while maintaining a level attitude, or even an orientation counter to the direction of motion, means that the OmniCopter can dock with or land on a moving feature while at the appropriate roll and pitch angle. A traditional multirotor or helicopter would need to maintain an angle proportional to its forwards velocity, which would make even landing on a moving horizontal surface challenging due to the forwards-tilt required to maintain forwards motion.



(a) Position vs. time.



(b) Velocity vs. time.

Figure 4.15: Matching a moving goal position.

# Chapter 5

## Conclusions and Recommendations for Future Work

As part of a larger project for aerial inspection, construction, and maintenance of industrial structures, a UAV was required which could support equipment and application as an aerial mobile manipulator base. UAVs in these applications experience unpredictable aerodynamic forces due to the proximity of structures and must be capable of resisting forces and torques which arise from use of the manipulator and physical contact with the environment. Since traditional multirotors and helicopters have limitations due to the coupling of orientation and translation, a novel UAV concept was required.

A multirotor based on a novel rotor layout was developed to satisfy the requirements of aerial mobile manipulation. This concept was dubbed the OmniCopter. The OmniCopter features the addition of four orthogonal thrust rotors to a traditional quadrotor layout. The addition of these rotors gives the OmniCopter the ability to generate forces in any axis independently of its orientation. It also features redundant control of torque along the X and Y axes, giving it the potential to tolerate the failure of

some rotors.

Tests were conducted on two types of rotors to quantify their thrust characteristics. The relationship between angular velocity and thrust, and ESC PWM signal and thrust was measured. It was discovered that for the orthogonal thrust rotors the quadratic model for angular velocity and thrust did not hold, potentially due to rotor blade deformation at higher RPM. The rate of change of thrust over time was measured and it was found that it took one second for the thruster to change from maximum forward thrust to maximum reverse thrust.

A system was developed for testing the autonomous control of UAVs which transmitted control signals generated by a PC through an RC transmitter. This system allowed a human operator to take manual control of the UAV at any time, thereby reducing the frequency of crashes. A prototype OmniCopter was constructed and tested using this system. The OmniCopter prototype was tested for its ability to resist unpredictable aerodynamic disturbances by generating simulated gusting winds with a large fan. It was found that in comparison to a traditional method of flight using roll and pitch for control, the OmniCopter was able to resist disturbances slightly better.

The OmniCopter prototype also demonstrated the ability to hover while maintaining a tilt angle of up to 20 degrees. This type of motion would be impossible for a traditional multirotor or helicopter and allows the OmniCopter greater flexibility when maneuvering. It allows the possibility to do things like perch on non-horizontal landing features and position on-board equipment optimally relative to the environment. The OmniCopter prototype demonstrated autonomously flying to and landing on a surface inclined by 30 degrees by matching the tilt of the surface. Furthermore, by

adding an input for goal velocity to the control algorithm, it was demonstrated that the OmniCopter could match the velocity of a moving target. This, combined with the ability to fly at non-standard orientations, means that the OmniCopter is more capable of landing on or docking with moving vehicles than traditional multirotors, which are limited by the need to maintain a tilt proportional to their velocity.

Overall, a UAV concept was developed and a prototype constructed which overcomes the limitations traditional multirotors and helicopters in aerial mobile manipulation applications.

## 5.1 Recommendations Future Work

There are several areas for further development of the OmniCopter UAV and the larger scope AMS, which includes the lifting-gas airship, umbilical cord, lightweight manipulator system, and docking system. On the OmniCopter itself the areas for future work include:

- Use of variable pitch, larger diameter, and more powerful thrusters with stiffer propellers to further examine improvements in disturbance rejection.
- Generation of achievable trajectories and subsequent control of UAV acceleration instead of velocity.
- Transfer of all processing and control tasks to on-board the OmniCopter.
- On-board localization.
- Fully omni-directional flight, demonstrating changing orientation arbitrarily during controlled translational flight.
- Investigation of rotor redundancy and recovery from rotor failures.

Areas for future work in the greater scope of the AMS project include:

- Development of an autonomous high endurance lifting-gas airship with a high payload capacity.
- Development of the umbilical cord system such that large power transfer is possible over long cables.
- Management of umbilical cord cable slack and cable positioning.
- Development and integration of a light-weight manipulator system with the OmniCopter.
- Development of a docking mechanism and docking algorithms.

# References

- [1] J. J. Craig, *Introduction to Robotics: Mechanics and Control*, 3rd ed. New Jersey: Prentice Hall, 2005.
- [2] K. Dalamagkidis, “Definitions and Terminology,” in *Handbook of Unmanned Aerial Vehicles*. Dordrecht: Springer Netherlands, 2015, pp. 43–55. [Online]. Available: [http://link.springer.com/10.1007/978-90-481-9707-1\\_92](http://link.springer.com/10.1007/978-90-481-9707-1_92)
- [3] S. Howeth, “Radio Controlled Aircraft,” pp. 479–493, 1963. [Online]. Available: <http://earlyradiohistory.us/1963hw40.htm>
- [4] T. Baltovski, S. B. Nokleby, and R. Pop-Iliev, “Design and Development of an Swinging Arm Mechanism for an Aerial Manipulator System,” in *Proceedings of the International Conference on Mechanical Engineering and Mechatronics*, Toronto, Canada, aug 2013, p. 7 pages.
- [5] T. Baltovski S.B. Nokleby and R. Pop-Iliev, “Towards Performing Remote Manipulation Using an Autonomous Aerial Vehicle,” in *Proceedings of the 2015 CCToMM Symposium on Mechanisms, Machines, and Mechatronics*, Ottawa, Canada, may 2015, p. 12 pages.
- [6] K. Dalamagkidis, “Classification of UAVs,” in *Handbook of Unmanned Aerial Vehicles*. Dordrecht: Springer Netherlands, 2015, pp. 83–91. [Online]. Available: [http://link.springer.com/10.1007/978-90-481-9707-1\\_94](http://link.springer.com/10.1007/978-90-481-9707-1_94)

- [7] S. Bouabdallah, P. Murrieri, and R. Siegwart, “Design and control of an indoor micro quadrotor,” in *IEEE International Conference on Robotics and Automation, 2004. Proceedings. ICRA '04. 2004*, vol. 5. IEEE, 2004, pp. 4393–4398 Vol.5. [Online]. Available: <http://ieeexplore.ieee.org/lpdocs/epic03/wrapper.htm?arnumber=1302409>
- [8] G. Morgenthal and N. Hallermann, “Quality assessment of unmanned aerial vehicle (UAV) based visual inspection of structures,” *Advances in Structural*, 2014. [Online]. Available: <http://ase.sagepub.com/content/17/3/289.short>
- [9] L. F. Luque-Vega, B. Castillo-Toledo, A. Loukianov, and L. E. Gonzalez-Jimenez, “Power line inspection via an unmanned aerial system based on the quadrotor helicopter,” in *MELECON 2014 - 2014 17th IEEE Mediterranean Electrotechnical Conference*. IEEE, apr 2014, pp. 393–397. [Online]. Available: <http://ieeexplore.ieee.org/lpdocs/epic03/wrapper.htm?arnumber=6820566>
- [10] A. Gibiansky, “Quadcopter Dynamics , Simulation , and Control Introduction Quadcopter Dynamics,” pp. 1–18, 2012. [Online]. Available: <http://andrew.gibiansky.com/blog/physics/quadcopter-dynamics/>
- [11] B. Erginer and E. Altug, “Modeling and PD Control of a Quadrotor VTOL Vehicle,” in *2007 IEEE Intelligent Vehicles Symposium*. IEEE, jun 2007, pp. 894–899. [Online]. Available: <http://ieeexplore.ieee.org/lpdocs/epic03/wrapper.htm?arnumber=4290230>
- [12] A. Tayebi and S. McGilvray, “Attitude stabilization of a VTOL quadrotor aircraft,” *IEEE Transactions on Control Systems Technology*, vol. 14, no. 3, pp. 562–571, may 2006. [Online]. Available: <http://ieeexplore.ieee.org/lpdocs/epic03/wrapper.htm?arnumber=1624481>
- [13] D. Mellinger, Q. Lindsey, and M. Shomin, “Design, modeling, estimation and

- control for aerial grasping and manipulation,” *2011 IEEE/RSJ*, 2011. [Online]. Available: [http://ieeexplore.ieee.org/xpls/abs{\\\_}all.jsp?arnumber=6094871](http://ieeexplore.ieee.org/xpls/abs{\_}all.jsp?arnumber=6094871)
- [14] S. Bouabdallah and R. Siegwart, “Backstepping and Sliding-mode Techniques Applied to an Indoor Micro Quadrotor,” in *Proceedings of the 2005 IEEE International Conference on Robotics and Automation*. IEEE, 2005, pp. 2247–2252. [Online]. Available: <http://ieeexplore.ieee.org/lpdocs/epic03/wrapper.htm?arnumber=1570447>
- [15] J. Dunfield, M. Tarbouchi, and G. Labonte, “Neural network based control of a four rotor helicopter,” in *2004 IEEE International Conference on Industrial Technology, 2004. IEEE ICIT '04.*, vol. 3. IEEE, 2004, pp. 1543–1548. [Online]. Available: <http://ieeexplore.ieee.org/lpdocs/epic03/wrapper.htm?arnumber=1490796>
- [16] T. Madani and A. Benallegue, “Backstepping Control for a Quadrotor Helicopter,” in *2006 IEEE/RSJ International Conference on Intelligent Robots and Systems*. IEEE, oct 2006, pp. 3255–3260. [Online]. Available: <http://ieeexplore.ieee.org/lpdocs/epic03/wrapper.htm?arnumber=4058900>
- [17] A. Benallegue, A. Mokhtari, and L. Fridman, “Feedback Linearization and High Order Sliding Mode Observer For A Quadrotor UAV,” in *International Workshop on Variable Structure Systems, 2006. VSS'06.* IEEE, 2006, pp. 365–372. [Online]. Available: <http://ieeexplore.ieee.org/lpdocs/epic03/wrapper.htm?arnumber=1644545>
- [18] S. Waslander, G. Hoffmann, Jung Soon Jang, and C. Tomlin, “Multi-agent quadrotor testbed control design: integral sliding mode vs. reinforcement learning,” in *2005 IEEE/RSJ International Conference on Intelligent Robots and Systems*. IEEE, 2005, pp. 3712–3717. [Online]. Available: <http://ieeexplore.ieee.org/lpdocs/epic03/wrapper.htm?arnumber=1545025>

- [19] G. Chowdhary, T. Wu, M. Cutler, N. K. Ure, and J. How, “Experimental Results of Concurrent Learning Adaptive Controllers,” in *AIAA Guidance, Navigation, and Control Conference*. Reston, Virigina: American Institute of Aeronautics and Astronautics, aug 2012. [Online]. Available: <http://arc.aiaa.org/doi/abs/10.2514/6.2012-4551>
- [20] H. Lee, S. Kim, and H. Kim, “Control of an aerial manipulator using on-line parameter estimator for an unknown payload,” *2015 IEEE International Conference on*, 2015. [Online]. Available: [http://ieeexplore.ieee.org/xpls/abs\\_all.jsp?arnumber=7294098](http://ieeexplore.ieee.org/xpls/abs_all.jsp?arnumber=7294098)
- [21] G. Heredia, A. Jimenez-Cano, and I. Sanchez, “Control of a multirotor outdoor aerial manipulator,” *2014 IEEE/RSJ*, 2014. [Online]. Available: [http://ieeexplore.ieee.org/xpls/abs\\_all.jsp?arnumber=6943038](http://ieeexplore.ieee.org/xpls/abs_all.jsp?arnumber=6943038)
- [22] D. Mellinger and V. Kumar, “Minimum snap trajectory generation and control for quadrotors,” in *Proceedings - IEEE International Conference on Robotics and Automation*. IEEE, may 2011, pp. 2520–2525. [Online]. Available: <http://ieeexplore.ieee.org/lpdocs/epic03/wrapper.htm?arnumber=5980409>
- [23] C. Richter, A. Bry, and N. Roy, “Polynomial trajectory planning for aggressive quadrotor flight in dense indoor environments,” *Robotics Research*, 2016. [Online]. Available: [http://link.springer.com/chapter/10.1007/978-3-319-28872-7\\_37](http://link.springer.com/chapter/10.1007/978-3-319-28872-7_37)
- [24] V. Hrishikeshavan, J. Black, and I. Chopra, “Development of a Quad Shrouded Rotor Micro Air Vehicle and Performance Evaluation in Edgewise Flow,” *Journal of Aircraft*, vol. 49, 2012. [Online]. Available: <http://terpconnect.umd.edu/~vikramh/quadshroud/hoverandedgewiseflowperformance.pdf>
- [25] P. Pounds, R. Mahony, J. Gresham, P. Corke, and J. M. Roberts, “Towards dynamically-favourable quad-rotor aerial robots,” *Faculty of Built Environment*

*and Engineering; Institute for Future Environments; School of Engineering Systems*, 2004.

- [26] S. Kittiyoungkun, “Aerodynamic problems of urban UAV operations,” *Cranfield University*, no. August, 2010. [Online]. Available: <http://dspace.lib.cranfield.ac.uk/handle/1826/6158>
- [27] P. Pounds and A. Dollar, “Aerial grasping from a helicopter UAV platform,” *Experimental Robotics*, 2014. [Online]. Available: [http://link.springer.com/chapter/10.1007/978-3-642-28572-1\\_{\\_}19](http://link.springer.com/chapter/10.1007/978-3-642-28572-1_{_}19)
- [28] V. Powers, C., Mellinger, D., Kushleyev, A., Kothmann, B., Kumar, “Experimental Robotics,” *ISER, June*, vol. 88, no. 287513, pp. 515–529, 2013. [Online]. Available: [http://link.springer.com/10.1007/978-3-319-00065-7\\_{\\_}21](http://link.springer.com/10.1007/978-3-319-00065-7_{_}21)<http://link.springer.com/10.1007/978-3-319-00065-7>
- [29] C. Doyle, J. Bird, T. Isom, and C. Johnson, “Avian-inspired passive perching mechanism for robotic rotorcraft,” *2011 IEEE/RSJ*, 2011. [Online]. Available: [http://ieeexplore.ieee.org/xpls/abs{\\_}all.jsp?arnumber=6094487](http://ieeexplore.ieee.org/xpls/abs{_}all.jsp?arnumber=6094487)
- [30] D. Mellinger, M. Shomin, N. Michael, and V. Kumar, “Cooperative grasping and transport using multiple quadrotors,” in *Springer Tracts in Advanced Robotics*, vol. 83 STAR. Springer Berlin Heidelberg, 2012, pp. 545–558. [Online]. Available: [http://link.springer.com/10.1007/978-3-642-32723-0\\_{\\_}39](http://link.springer.com/10.1007/978-3-642-32723-0_{_}39)
- [31] P. I. T. M. Das, S. Swami, and J. M. Conrad, “An algorithm for landing a quadrotor unmanned aerial vehicle on an oscillating surface,” in *Conference Proceedings - IEEE SOUTHEASTCON*, 2012. [Online]. Available: [http://ieeexplore.ieee.org/xpls/abs{\\_}all.jsp?arnumber=6196934](http://ieeexplore.ieee.org/xpls/abs{_}all.jsp?arnumber=6196934)
- [32] G. Jiang, “Dextrous Hexrotor UAV Platform,” Master’s thesis, University of Denver, 2013.

- [33] R. Cano, C. Pérez, F. Pruano, and A. Ollero, “Mechanical design of a 6-DOF aerial manipulator for assembling bar structures using UAVs,” *2nd RED-UAS 2013*, 2013. [Online]. Available: <http://www.arcas-project.eu/sites/default/files/MechanicalDesignofa6-DOFAerialManipulatorforassemblingbarstructuresusingUAVs.pdf>
- [34] A. Albers, S. Trautmann, and T. Howard, “Semi-autonomous flying robot for physical interaction with environment,” *on Robotics*, . . ., 2010. [Online]. Available: <http://ieeexplore.ieee.org/xpls/abs{ }all.jsp?arnumber=5513152>
- [35] D. Langkamp, G. Roberts, and A. Scillitoe, “An engineering development of a novel hexrotor vehicle for 3D applications,” *Micro Air Vehicle* . . ., 2011. [Online]. Available: <http://repository.tudelft.nl/view/conferencepapers/uuid:d7bdec21-938d-426b-9553-59cf834e8061/>
- [36] Y. Long and D. J. Cappelleri, “Omnicopter: A Novel Overactuated Micro Aerial Vehicle,” in *Advances in Mechanisms, Robotics and Design Education and Research*, 2013, pp. 215–216. [Online]. Available: <http://link.springer.com/10.1007/978-3-319-00398-6{ }16>
- [37] S. Salazar, H. Romero, R. Lozano, and P. Castillo, “Modeling and Real-Time Stabilization of an Aircraft Having Eight Rotors,” *Journal of Intelligent and Robotic Systems*, vol. 54, no. 1-3, pp. 455–470, mar 2009. [Online]. Available: <http://link.springer.com/10.1007/s10846-008-9274-x>
- [38] D. Brescianini and R. D’Andrea, “Design , Modeling and Control of Omni-Directional Aerial Robot,” *IEEE International Conference on Robotics and Automation*, 2016.
- [39] D. G. Lee and N. P. Suh, *Axiomatic Design and Fabrication of Composite Structures*. Oxford University Press, 2006.

- [40] E. Rimon and J. Burdick, “On force and form closure for multiple finger grasps,” . . . ., 1996 IEEE International Conference on, vol. 2, no. April, pp. 1795–1800, 1996. [Online]. Available: <http://ieeexplore.ieee.org/lpdocs/epic03/wrapper.htm?arnumber=506972>  
[http://ieeexplore.ieee.org/lpdocs/epic03/wrapper.htm?arnumber=506972\\$\\delimiter"026E30F\\$nhhttp://ieeexplore.ieee.org/xpls/abs{\\_-}all.jsp?arnumber=506972](http://ieeexplore.ieee.org/lpdocs/epic03/wrapper.htm?arnumber=506972$\\delimiter)
- [41] Z. Li. (2014, feb) ROS mocap. [Online]. Available: [http://wiki.ros.org/mocap{\\_-}optitrack](http://wiki.ros.org/mocap{_-}optitrack)
- [42] I. Saito. (2015, jul) ROS tf. [Online]. Available: <http://wiki.ros.org/tf>